

Electronic Thesis and Dissertation Repository

---

8-20-2012 12:00 AM


## Synthesis of silicide nanomaterials using chemical vapour deposition method

Hamid Norouzi Banis  
*The University of Western Ontario*

Supervisor  
Dr. Andy Xueliang Sun  
*The University of Western Ontario*

Graduate Program in Mechanical and Materials Engineering  
A thesis submitted in partial fulfillment of the requirements for the degree in Master of Engineering Science  
© Hamid Norouzi Banis 2012

Follow this and additional works at: <https://ir.lib.uwo.ca/etd>

 Part of the [Materials Chemistry Commons](#), and the [Nanoscience and Nanotechnology Commons](#)

---

### Recommended Citation

Norouzi Banis, Hamid, "Synthesis of silicide nanomaterials using chemical vapour deposition method" (2012). *Electronic Thesis and Dissertation Repository*. 767.  
<https://ir.lib.uwo.ca/etd/767>

This Dissertation/Thesis is brought to you for free and open access by Scholarship@Western. It has been accepted for inclusion in Electronic Thesis and Dissertation Repository by an authorized administrator of Scholarship@Western. For more information, please contact [wlsadmin@uwo.ca](mailto:wlsadmin@uwo.ca).

# **Synthesis of silicide nanomaterials using chemical vapour deposition method**

(Spine title: Synthesis of NiSi<sub>x</sub> and CoSi nanomaterial)

(Thesis format: Integrated)

By

Hamid Norouzi Banis

Graduate Program in Mechanical and Materials Engineering

A thesis submitted in partial fulfillment  
of the requirements for the Degree of  
Masters of Science

The School of Graduate and Postdoctoral Studies  
The University of Western Ontario  
London, Ontario, Canada

©Hamid Norouzi Banis 2012

THE UNIVERSITY OF WESTERN ONTARIO  
SCHOOL OF GRADUATE AND POSTDOCTORAL STUDIES

**CERTIFICATE OF EXAMINATION**

Supervisor

\_\_\_\_\_  
Dr. Xueliang (Andy) Sun

Supervisory Committee

\_\_\_\_\_  
Dr. Robert Klassen

Examiners

\_\_\_\_\_  
Dr. Liying Jiang

\_\_\_\_\_  
Dr. T. Kuboki

\_\_\_\_\_  
Dr. Jin Zhang

The thesis by

**Hamid Norouzi Banis**

entitled:

**Synthesis of silicde nanomaterials using chemical vapour deposition  
method**

is accepted in partial fulfillment of the

requirements for the degree of

Master of Science

Date August 20/2012

Dr. George K. Knopf \_\_\_\_\_

Chair of the Thesis Examination Board

## Abstract

Recent research has evidenced that nanotechnology may bring about a material revolution which sweeps through different scientific fields and leads to dramatic changes in the use of natural resources and our everyday life. Compared to their bulk counterparts, the nanomaterials may exhibit significantly improved physical properties by shrinking their size to nanometer scale. Metal silicide are distinguished by their features of combining advantages of both metals and semiconductors which promises superior performance various fields. Despite the progress in the synthesis methods of nanomaterials, it still remains a big challenge in controlled synthesis of 1D silicide nanostructures due to the difficulties of well-controlled synthesis conditions.

In this study, synthesis process of  $\text{NiSi}_x$  and  $\text{CoSi}_x$  with different morphologies using CVD method have been analysed and determined. Synthesis of different structures of  $\text{NiSi}_x$  on a number of substrates has been investigated. The mechanisms behind the growth of these nanostructures have been studied for better understanding of the synthesis of these silicides. The detailed characterization techniques such as SEM, TEM and XRD were used.

**Keywords:** Nanomaterial, Chemical Vapor deposition, Metal Silicide.

## **Dedication**

I thank God for all he has given me and I dedicate this thesis to my lovely family, my father and mother who have always supported me in all the stages of my studies and in difficulties that I have had. To my brother Mohammad without whom I could not have been able to learn and carry out my work this fast and well. His support has always given me strength and confidence so I could be at my best.

## ACKNOWLEDGMENTS

This master thesis was carried out in Dr. Sun's nanomaterial and Clean Energy Lab at University of Western Ontario (UWO), Canada. In the two years that I have spent in Dr. Sun's group I have met and worked with great people that have helped me in different steps of my studies.

Firstly, I would like to thank Dr. Xuelaing Sun for accepting me in his group and for all the efforts that he put on my work and studies. He had guided all through my work and gave help to me through many different ways which gave me a remarkable experience. His patience and strong support always encouraged me to move forward and be persistent on my efforts. He truly has been an example for me in many ways which hopefully I would be able to adapt those characters in myself.

I am also very grateful that we had an amazing research engineer and technician Mrs. Ruying (Kathy) Li in our group. Her management of the labs and organizations is why the members of this group can work so efficiently and easily. Besides teaching me a lot about nanomaterials and characterization, she always treated me with kindness and respect. I hope she would always be doing well and her family to be successful in all aspects of life.

I would like to thank my brother Mohammad Norouzi Banis, a PhD student in Dr. Sun's lab, who taught me and guided me in all the stages of my work. I always felt so blessed to have him working alongside me and supporting me thorough the challenges that I had faced. Without him, the tasks would not have been finished and problems wouldn't have been solved this smoothly. I will always be in debt to my older brother.

I also have to thank Dr. Yong (Bryan) Zhang for all the efforts and time he put in

helping me in many different aspects of my research and thesis. Despite having extensive amount of work on his own hands, he always would spare some time for my work as well. I am truly grateful his kindness.

Many thanks to my wonderful group members in Dr. Sun's lab, Xifei Li ,Yuhai Hu, Yongliang Li, Dongsheng Geng, Jian Liu, Jinli Yang, Dongniu Wang, Shuhui Sun, Gaixia Zhang, Jiajun Wang, Liang Li, Yongji Tang, Dr Mihnea Ioan Ionescu. I t was a pleasure being in a group of hard working and pleasant people. It has been the help and collaboration of these people that has brought me here.

With Best Regards,

Hamid Norouzi Banis

# Table of Contents

<b>Abstract.....</b>	<b>ii</b>
<b>Acknowledgment .....</b>	<b>iv</b>
<b>List of Figures .....</b>	<b>vii</b>
<b>List of Tables.....</b>	<b>xii</b>
<b>Chapter 1 Literature Review.....</b>	<b>1</b>
1.1. Nanomaterials.....	1
1.1.1. Introduction.....	1
1.1.2. One dimensional nanomaterials.....	3
a. Nanotubes.....	3
b. Nanowires.....	4
1.1.3. Synthesis methods for nanowire growth.....	5
1.1.4. Mechanism for vapor-phase growth of nanowires.....	6
a. Vapour-liquid-solid growth .....	7
b. Vapour-solid growth.....	9
c. Oxide assisted growth.....	10
d. Solid-liquid-solid growth.....	10
1.2. Silicide nanostructures.....	12
1.2.1. Synthesis of silicide nanostructures.....	16
1.3. Applications.....	27
1.4. Thesis Outline and Objectives.....	31
References.....	34
<b>Chapter 2. Experimental and Characterization Techniques.....</b>	<b>38</b>
2.1. Chemical vapor deposition.....	38
2.1.1. NiSi <sub>x</sub> nanostructures.....	39
2.1.2. CoSi nanostructures .....	41
2.2. Characterization methods.....	42
2.2.1. Scanning Electron Microscope.....	42
2.2.2. Transmission Electron Microscope.....	46
2.2.3. X-ray Diffraction.....	48
References.....	49



<b>Chapter 3. Controlled Synthesis and Growth Mechanisms of NiSi<sub>x</sub> Nanowires by Chemical Vapor Deposition .....</b>	<b>50</b>
3.1. Introduction.....	50
3.2. Experimental procedure.....	52
3.3. Results and discussions .....	53
3.3.1. Temperature effect.....	57
3.3.2. Substrate effect .....	59
3.3.3. Growth mechanism.....	61
3.4. Conclusion.....	64
References .....	65
<b>Chapter 4. Synthesis of CoSi Nanowires Using Chemical Vapor Deposition at Different Ambient Pressure Levels .....</b>	<b>67</b>
4.1. Introduction.....	67
4.2. Experimental procedure.....	69
4.3. Results and discussions .....	70
4.3.1. Temperature effect.....	74
4.3.2. Growth mechanism.....	79
4.4. Conclusion.....	81
References .....	82
<b>Chapter 5. Conclusion and Future work .....</b>	<b>84</b>
<b>Curriculum Vitae.....</b>	<b>87</b>

# List of Figures

## Chapter 1

Figure 1.1 a) SEM image of a large product of carbon nanotubes; b) schematics of a single wall carbon nanotube.....	4
Figure 1.2. SEM image of copper nanowires.....	5
Figure 1.3 Ge-Au Binary phase diagram [10].....	7
Figure 1.4 Schematic diagram of Ge nanowire grown using VLS mechanism [10]. .....	8
Figure 1.5 Schematic diagram of Si nanowire synthesized using Ni catalyst via SLS growth mechanism [21] .....	11
Figure 1.6 (a) The schematics of the spontaneous nanowire growth in this study. (b-d) The representative SEM images of the reaction products on H <sub>2</sub> -, N <sub>2</sub> -, and O <sub>2</sub> -annealed samples, respectively. Scale bar 1µm.....	17
Figure 1.7. Top-view SEM image of nanowires, 950 °C, 16 h, a) FeSi <sub>2</sub> film on Si, the dark contrast regions correspond to the pinholes. Upper inset shows a side-view SEM image. The bottom inset shows side-view SEM image of a pinhole, b) FeSi <sub>2</sub> nanodots on Si. Upper inset shows a side-view SEM image. ....	19
Figure 1.8. Experimental setup. (a) Horizontal tube furnace with two independently controlled heating zones. (b) Temperature profile indicates that the center of the downstream zone is at 900 °C, and the substrates are at 820-890 °C. (c) Tilted view illustration of the substrate placement in panel a. A rectangular Si wafer (50mm-150 mm) kept at the downstream zone played a role of Si source for NW synthesis. Co <sub>2</sub> Si NWs are grown on the sapphire 1 substrate, CoSi NWs on the Si, and Co <sub>3</sub> Si NWs on the sapphire 2.....	21
Figure 1.9 Synthesis of metal silicide NWs using chemical vapour transport (CVT). Silicides undergo reversible reaction with I <sub>2</sub> at T <sub>1</sub> to form in situ gas phase products. At T <sub>2</sub> gas phase components undergo the reverse reaction to form silicide NWs. ....	24

Figure 1.10 Synthesis of metal silicide NWs using chemical vapour deposition (CVD) of single source precursors (SSP). Each SSP pyrolyzes to deliver metal silicide material to the growth substrate. ....	25
Figure 1.11 Preparation of NiSi NWs by silicidation. a1) Si NWs (blue) are synthesized via VLS and a2) coated with Ni metal (green), a3) reacted at 550 °C to form NiSi nanowires (orange). a4) Extra Ni metal is etched away leaving single crystalline NiSi NWs.62 b) Preparation of NiSi NWs by point contact silicidation to form NiSi–Si NW heterostructures. ....	27
Figure 1.12 Two-probe (1) and four-probe (2) electrical transport for single Ni <sub>2</sub> Si NWs	29
Figure 1.13 (a), (b) Top-view SEM images of the Ni silicide nanosheets (c) Electrochemical performance of the Ni silicide nanosheets (comprising Ni <sub>3</sub> Si and Ni <sub>31</sub> Si <sub>12</sub> ) grown on a Ni foil substrate and of the Ni silicide nanobelts (Ni <sub>3</sub> Si) grown on a Ni foam substrate. ....	31

## Chapter 2

Figure 2.1 Schematic diagram of CVD method used for the synthesis of NiSi nanostructures. ....	38
Figure 2.2 Schematic diagram showing the setup of substrate and the sources in Quartz tube of CVD process for the synthesis of NiSix nanowires.....	39
Figure 2.3 Schematic diagram showing the setup of substrate and the sources in Quartz tube of CVD process for the synthesis of CoSi nanowires. ....	41
Figure 2.4 A photo of our SEM (Hitachi S-4800) .....	42
Figure 2.5 A schematic drawing of the electron and X-ray optics on a combined SEM-EPMA [1]......	44
Figure 2.6 A schematic of a TEM [2]......	45
Figure 2.7 A photo of our TEM (Philip CM10)......	46
Figure 2.8 A photo of Bruker D8 Advance XRD [3]......	47

## Chapter 3

- Figure 3.1 Schematic diagram of the nickel silicide synthesis process .....52
- Figure 3.2 HRSEM image of Ni<sub>2</sub>Si nanowires. (a) low magnification (a) High magnification (b)cross section view. the thickness of the bundles are around 5-10 um (c) XRD pattern of these nanowires on a silicon substrate. ....53
- Figure 3.3 (a) TEM image of a single Ni<sub>2</sub>Si nanowire with a diameter of about 250 nm. ((b) Corresponding SAED pattern (c) HRTEM of the NW and EDX analysis of these nanowires (inset). ....55
- Figure 3.4 SEM and EDX spectrum of nanostructures synthesized on silicon wafer at (a, b) 850 °C (c, d) 900 °C (e, f) 950 °C. ....57
- Figure 3.5 SEM and XRD pattern of NiSix NWs growth on (a, b) carbon paper (c,d) Ni foam. ....59
- Figure 3.6 (a) Schematic diagram of the NW heterostructures growth. HRSEM image of time dependent growth of nanostructures: (b) 30min; (c) 1hr; (d) 1:15hr; (f) 1:45hr. ....61

## Chapter 4

- Figure 4.1 Schematic diagram showing the setup of substrate and the sources in Quartz tube of CVD process for the synthesis of CoSi nanowires. ....68
- Figure 4.2 (a) HRSEM at 850 °C in atmospheric condition; (b) XRD pattern; (c) TEM image of single nanowire; (d) HRTEM of CoSi nanowire (inset is SAED pattern)..... 70
- Figure 4.3 (a) HRSEM at 900 °C at 10 Torr; (b) XRD pattern; (c) TEM image of single nanowire; (d) HRTEM of CoSi nanowire (inset is SAED pattern). ....72
- Figure 4.4 Representative High magnification SEM image (inset is low magnification) of CoSi nanowires synthesized in atmospheric condition at (a) 850 °C , (b) 900 °C and (c) 930°C respectively. at 10 Torr (b) EDX spectrum of products synthesized at (d) 850°C , (e)900°C (f) 930°C .....74

Figure 4.5 Representative High magnification SEM image (inset is low magnification) of CoSi nanowires synthesized in 1mbar ambient pressure at (a) 850oC , (b) 900oC and (c) 930oC respectively. at 10 Torr (b) EDX spectrum of products synthesized at (d) 850oC , (e) 900°C(f)930°C .....77

Figure 4.6 (a) low magnification TEM image of CoSi nanowire with a nanoparticle; (b) High Resolution TEM image of the catalyst nanoparticle; (c) EDX spectra of the nanoparticle. ....79

## List of Tables

### Chapter1

Table 1. Typical dimensions of nanomaterials along with examples of material used in these types of groups for various applications [4] .....	2
Table 2 Periodic table of the transition metal silicide phases [26] .....	15

## Chapter 2 Introduction

### 1.1. Nanomaterials

#### 1.1.1. Introduction

Nanomaterials are one of the building blocks of nanotechnology. Depending on the application and purpose of nanomaterials, they have found various definitions. But they can be generally defined as materials with physical structures which at least one of their dimensions is between 1-100 nm [1]. Nanomaterial research is one of the fastest growing areas in materials science and engineering [2]. These materials have distinctly different physical and chemical properties from those of a single atom (molecule) and bulk matter with the same chemical composition. This is because many properties of solids depend on the size range over which they are measured. Microscopic details become averaged when investigating bulk materials. At the macro- or large scale traditional fields of physics such as mechanics, electricity and optics, the sizes of the objects under study range from millimeters to kilometers. The properties of these materials are averaged properties, such as density and elastic moduli in mechanics, resistivity and magnetization in electricity and magnetism. When the sizes of the objects shrink to micrometer or nanometer scale, dramatic changes of the material properties are unveiled [1]. This is why some of the important issues in nanoscience relate to size effects, shape phenomena, quantum confinement and optical excitations of individual and coupled finite systems [3].

Based on the above definition of nanomaterials, they can be classified into three major groups [4-6].

- 1) Zero-dimensional (0D) nanomaterials
- 2) One-dimensional (1D) nanomaterials
- 3) Two-dimensional (2D) nanomaterials

Type of nanomaterial	Nanostructures	Size	Materials
0D	Quantum dots Nanocrystals Nanoparticles	Diam. 1-10 nm Diam. 1-100 nm	Metals, semiconductors, Magnetic material , Ceramic oxides
1D	Nanowires Nanorods Nanobelts Nanocables Nanotubes	Diam. 1-100 nm	Metals , semiconductors oxides, sulfides, nitrides Carbon, layered metal chalcogenides
2D	Thin films	Thickness 1-1000 nm	A variety of material

**Table 1. Typical dimensions of nanomaterials along with examples of material used in these types of groups for various applications [4]**

Table 1 summarizes different types of nanomaterials in each category of these nanostructures. As shown, nanomaterials in each category come in wide range of dimensions and have numerous compositions and many studies have focused on the synthesis, characterization and application of these materials. In this study we will focus on one-dimensional nanostructures of silicide materials and their applications in Lithium ion batteries.



### **1.1.2. One-dimensional nanomaterials**

One-Dimensional nanomaterials might be the latest type of nanomaterials synthesized and studied for various applications compared to other types of nanomaterials. These structures have been given a variety of names including: whiskers, fibers or fibrils, nanowires and nanorods. In most cases, nanotubes and nanocables are also considered as 1D nanostructures. But generally 1D nanomaterials are divided into two major groups of nanotubes and nanowires.

#### **a. Nanotubes**

Nanotubes are 1D nanomaterials with hollow structures. There are many reports on the synthesis of organic and inorganic nanotubes [5]. Carbon nanotube is of the well know nanostructures in this group. Following the discovery of carbon nanotubes in 1991 [5] synthesis of these nanostructures have attracted tremendous attention due to their superior mechanical properties, unique electronic behaviour and their potential applications in various fields. These nanotubes are unique allotropes of carbon due to configuration of the carbon atoms that form the nanotube structure. A SEM image of a large yield of carbon nanotubes is shown in Fig. 1a. A schematic diagram for carbon nanotubes and the arrangements of the atoms can be clearly observed in the Fig. 1b. Carbon nanotubes possess many desirable properties, including high mechanical strength and flexibility, excellent electrical and thermal conductivity. These collective set of properties makes carbon nanotubes potential candidates for many applications including high strength composite materials, nanoscale transistors and fuel cell electrodes.

Recently there has been many reports of synthesis of other types of inorganic nanotubes such as titania nanotubes [6], Fe and its oxides [7-9], Si and SiO<sub>2</sub> and manganese oxide [10,11]. Compared to carbon nanotube studies, inorganic nanotubes started much later due to the difficulties in synthesizing these structures. Like carbon nanotubes, these inorganic nanotubes exhibit unique properties which makes them ideal candidates for various applications such as catalyst, energy technologies and electronics.

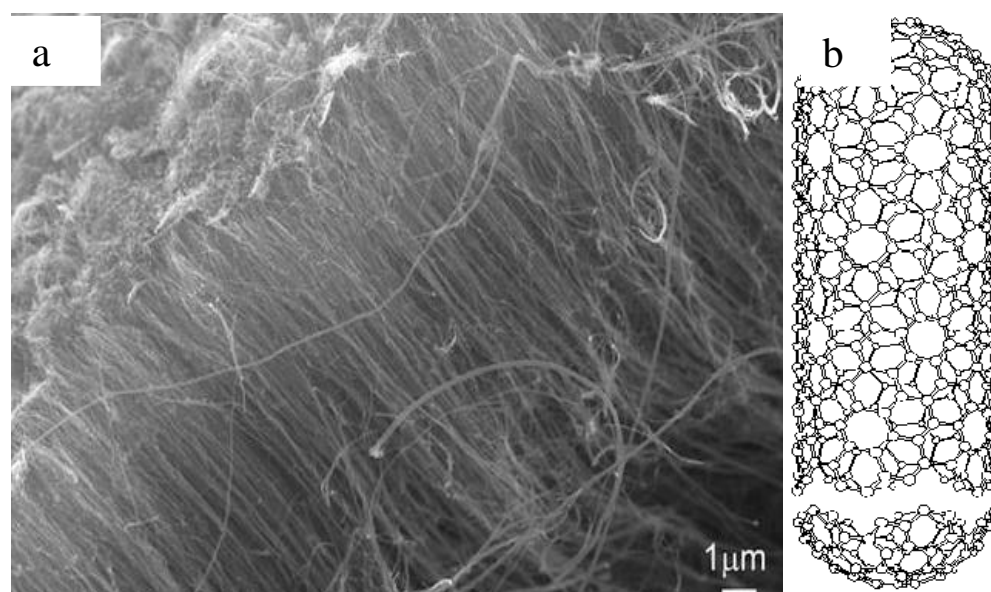


**Figure 2.1 a) SEM image of a large product of carbon nanotubes; b) schematics of a single wall carbon nanotube**

### **b. Nanowires**

Nanowires, nanorods and nanobelts constitute an important class of 1D nanostructures which provide models to study the relations between electrical transport, optical and other properties with dimensionality and size confinement. In comparison with quantum dots and carbon nanotubes, the advancement of these 1D nanostructures has been slow until very recently, as hindered by the difficulties associated with the synthesis of nanowires with well controlled dimension, morphology, phase purity and

chemical composition [12]. As an example SEM images of copper nanowires have been brought in Fig1.2 . As it is observed nanowires as opposed to nanotubes are not hollow inside. These structures can be crystalline or amorphous.

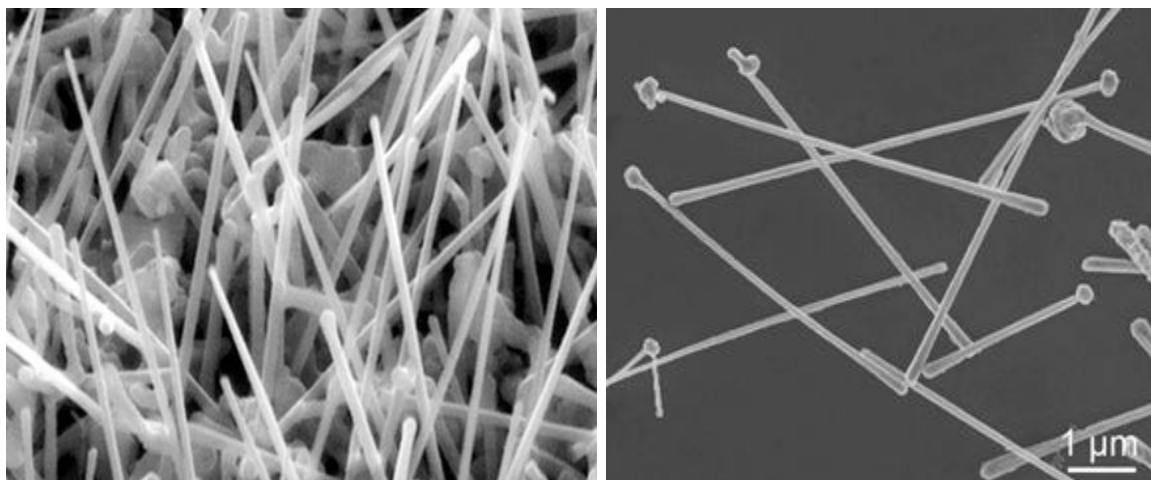


**Figure 2.2. SEM image of copper nanowires**

Nanowires are expected to play important roles as interconnects, functional components in the fabrication of nanoscale electronic and optoelectronic devices and electrochemical applications. Many studies have demonstrated the unique properties of nanowires and nanorods, such as superior mechanical toughness [13], high luminescence efficiency [14] and lower electrical resistance [15].

### **1.1.3. Synthesis methods for nanowire growth**

In order to study various properties of nanowires and their application in different fields and industries several challenges have to be addressed. The main challenges in application of nanomaterials are controlled synthesis with controlled size, morphology, microstructure and chemical composition. To do so, the increased understanding of growth mechanisms is critical.

Numerous methods have been reported for the synthesis of nanowires and various mechanisms have been proposed for these methods. Some of these methods include:

- Vapour deposition method
- Physical method(E- beam)
- Sol gel method
- Hydrothermal method
- Template method
- Wet chemical reduction

Each of these methods has some advantages and disadvantages depending on the composition and properties of nanomaterials, each method is used for producing certain types of nanowires. Among these methods, vapour deposition method is distinguished by its advantages such as low cost, fast synthesis, capability of mass or continuous production and control over certain aspects of nanomaterials synthesized. In this study we will focus on the synthesis method using vapour deposition method.

#### **1.1.4 Mechanism for vapour growth of nanowires**

Vapour phase growth is commonly used to produce nanowires, starting with simple evaporation technique in an appropriate atmosphere to produce elemental or oxide nanowires. To get insight into the growth of nanostructures via vapour phase methods and enhance the control over the deposited material, several mechanisms have been proposed. Vapour-liquid-solid (VLS), Vapour solid (VS), Solid-liquid-Solid (SLS) and Oxide assisted growth have been commonly recognized as the representative mechanisms.

### a. Vapor-liquid-solid growth (VLS)

The growth of nanowire via a gas phase reaction involving this process has been extensively studied. Wagner in 1960's, during his studies on the synthesis of large single crystalline whiskers, proposed this mechanism. According to this mechanism, the anisotropic crystal growth is promoted by the presence of a liquid alloy solid interface [15]. This mechanism was widely accepted and applied to understand the growth of various nanowires, such as Si and Ge. As an example, Xia et al [16] explained the growth of Ge nanowires using Au clusters as solvent at high temperatures based on the Ge-Au binary phase diagram (in Fig1.3).

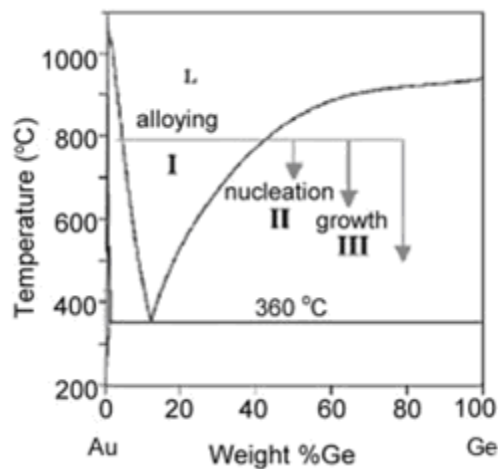


**Figure 2.3 Ge-Au Binary phase diagram [15]**

The schematic diagram of Ge nanowires grown using VLS mechanism is illustrated in Fig. 1.4 According to this diagram and Ge-Au binary phase diagram the Ge and Au will form a liquid alloy when the temperature is higher than the eutectic point. The liquid surface has a large accommodation coefficient and is therefore a preferred deposition site for incoming Ge vapour. After the liquid alloy becomes supersaturated

with Ge, the nanowire growth occurs by precipitation at the solid-liquid surface. A real time observation of Ge nanowire growth conducted in an *in situ* high temperature transmission electron microscope showed a sequence of TEM images which directly mirrors the proposed VLS mechanism. This VLS method has been exploited in the past several decades to produce 1-100  $\mu\text{m}$  diameter 1D structures (whiskers). By controlling the nucleation and growth it is possible to produce nanowires.

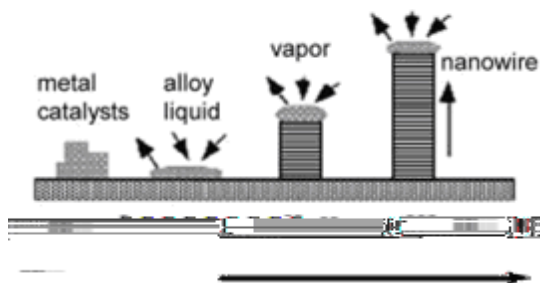


**Figure 2.4 Schematic diagram of Ge nanowire grown using VLS mechanism [15].**

The synthesis of nanowires based on this mechanism requires several conditions, including:

- 1) Catalyst and source material: by knowing the equilibrium phase diagram one can predict the catalyst material and growth conditions for the VLS approach.
- 2) Equipment to vaporize the source material and melt the catalyst

Nanowires grown by this method usually have certain features which help identify their growth mechanism. For example, most of nanowires synthesized using the VLS process have a catalyst droplet at their tip. But this is not always the case and depends on the interaction of liquid catalyst droplet with the substrate. There have been reports of nanowire

synthesized using VLS method with catalyst particles at the base of nanowires[17-19]. This is similar to growth process of carbon nanotubes.

### **b. Vapor-solid growth (VS)**

Besides VLS mechanism, the classical vapour solid method for whiskers growth has also been reported for the growth of 1D nanomaterials. In this process, the vapour is first generated by evaporation, chemical reduction or gaseous reaction. The vapour is subsequently transported and condensed onto a substrate. The VS method has been used to prepare oxide metal whiskers with micrometer diameters. Hence it is possible to synthesize 1D nanostructures if one can control its nucleation and subsequent growth process. Sears [11] ) was the first to explain the growth of mercury whiskers by axial screw dislocation induced anisotropic growth in 1955. The mercury whiskers or nanowire were grown by a simple VS method at  $-50\text{ }^{\circ}\text{C}$  under high vacuum. Subsequently a lot of research was devoted to studying the growth of nanostructures using this method and researchers revealed that the growth of nanorods or nanowires is not necessarily controlled by the presence of defects [12].

Usually nanowires and nanorods grown by VS method are single crystals with fewer impurities. The formation of 1D nanostructures through this method are due to anisotropic growth. Several mechanisms are proposed to explain the anisotropic growth. For example:

- 1) Different facets in a crystal have different growth rates.
- 2) Presence of impurities in specific crystal directions such as screw dislocation.
- 3) Preferential accumulation or poisoning by impurities on specific facets.

Also in case of synthesis of nanowires and nanorods, it is known that the impurities have differential adsorption on different crystal facets in a given crystal and the adsorption of impurity would retard the growth process. Impurity poisoning has often been cited as one of the reasons which resulted in anisotropic growth during synthesis of nanowire and nanorods [12].

Using this method, nanowires for oxides of Zn [13], Sn [14], In [15], Mg [16] and Ga [17] has been obtained .

### **c. Oxide assisted growth**

In contrast to the well-established VLS and VS mechanism, there have been reports of nanowire growth using different processes. One of these processes is oxide assisted nanowire growth. Lee et al. [30], reported the synthesis of GaAs nanowires by oxide assisted laser ablation of mixture of GaAs and  $\text{Ga}_2\text{O}_3$ . The GaAs nanowires have lengths up to tens of micrometers and diameter in the range 10-120 nm. The oxide assisted nanowire growth mechanism was further applied for production of various nanostructures such as Si and  $\text{SiO}_x$  [31] copper sulphide [18], boron [19] and MgO [20] nanowires. The nanowire growth via this process is not very clear and researchers have proposed various steps for the growth process depending on the materials.

### **d. Solid-liquid-solid growth**

In general, a high temperature is required in the growth of nanowires by methods mentioned above. Recently it has been reported that at these temperatures, another growth process can be activated called solid-liquid-solid (SLS). This process is similar to VLS



mechanism but doesn't fall in the category of vapour based approach for nanowire synthesis.

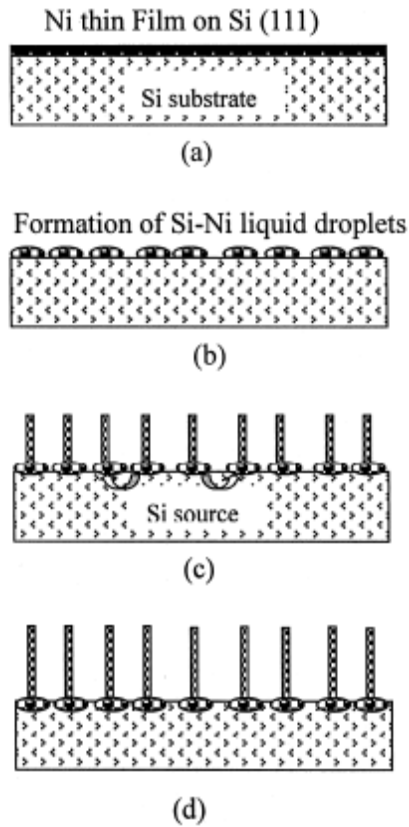


**Figure 2.5** Schematic diagram of Si nanowire synthesized using Ni catalyst via SLS growth mechanism [21]

There are few reports of synthesis of 1D nanostructures following SLS and mostly focus on silicon based material. Yan et al. [21], reported the synthesis of Si nanowires following this mechanism using Ni as catalyst.

They proposed that since the concentration of Si in the vapour phase was negligible at temperatures they carried out the experiments and because the substrate was covered only by a thin layer of Ni therefore the only possible silicon source was from the silicon substrate. Fig1.5 shows a schematic diagram of silicon nanowires grown using Ni as catalyst via SLS growth mechanism. They proved that the Ni layer reacts with Si substrate at high temperatures and from eutectic liquid alloy droplets and after super saturation of the droplets by silicon diffused through the substrate nanowires are synthesized [21].

There have been reports of other vapour based synthesis mechanism, such as carbothermal reactions which mostly based on the type of material. In this study both SLS and VLS mechanism have been the cause of the growth of the produced nanostructures which we will discuss in the next chapter.

## **1.2. Silicide Nanostructures**

Metal silicides, the family of refractory, intermetallic compounds between metals and silicon, have diverse physical properties that are both very useful and fundamentally significant. Metallic silicides [31,32] such as NiSi, CoSi<sub>2</sub>, and TiSi<sub>2</sub> provide ohmic contact, interconnect, and gate materials to CMOS microelectronic transistors. Semiconducting silicides have been extensively investigated for silicon-based optoelectronics such as LEDs and IR detectors. The narrow bandgap semiconducting silicides, in particular CrSi<sub>2</sub>, b-FeSi<sub>2</sub>, MnSi, and ReSi<sub>1.75</sub>, have been targeted for robust, stable, and inexpensive thermoelectric materials [33,34] and have shown promise for photovoltaic applications. In addition to finding numerous technological applications,

metal silicides have fascinated physicists for over 70 years and continue turning up surprises at the frontiers of theoretical and experimental condensed matter physics. The so-called B20 metal monosilicides (MSi, M= iron (Fe), cobalt (Co), manganese (Mn)) are a group of highly correlated electron materials. For example, FeSi is the only known transition metal Kondo insulator, a class of heavy-electron compounds exhibiting Kondo lattice behaviour at room temperature but having an insulating ground state with a small energy gap. MnSi, long thought of as a classical itinerant ferromagnet and the poster child of metal physics, has recently been discovered to have a quantum critical phase transition [22] and has been observed to exhibit non-Fermi liquid behaviour. These monosilicides and their alloys,  $\text{Fe}_{1-x-y}\text{Co}_x\text{Mn}_y\text{Si}$  ( $0 < x, y < 1$ ) also display a myriad of magnetic behaviours, including unusual helical magnetic ordering, [36,37] and even more exotic Skyrmion magnetic phases [23]. Furthermore,  $\text{Fe}_x\text{Co}_{1-x}\text{Si}$  alloys were recently discovered to be magnetic semiconductors, bringing exciting prospects of CMOS compatible silicon-based spintronics, a growing field that seeks to exploit the spin properties instead of or in addition to the charge degree of freedom in electronic and photonic devices [24].

Efforts thus far have concentrated on semiconductor channel materials, but metallic contact and gate materials are equally important for continued scaling of CMOS devices [40]. NWs of CMOS compatible metallic silicides having low resistivity and suitable work functions, such as nickel silicides [25], would serve as superior interconnect and gate contacts for nanoelectronic architectures. High quality single crystal semiconducting NWs, such as the half-metallic  $\text{Fe}_{1-x}\text{Co}_x\text{Si}$  alloys, will lay the nanomaterials foundation for the exploration of many technologically relevant fields. The rational synthesis of NWs from the vapour phase has two fundamental challenges [41,42]

- 1) delivery of source materials

2) anisotropic crystal growth to form 1-D nanostructures.

Free-standing transition metal silicide nanowire synthesis has been primarily limited by the lack of a general growth scheme such as in VLS grown semiconducting NWs (group IV elements and normal valence compounds such as the II–VI and III–V compounds) that exhibit simple phase behaviour with low melting eutectics that serve as a VLS catalytic system.

General and rational chemical synthesis of silicide nanomaterials is challenging, due in part to the multiple stoichiometries and complex phase behaviour exhibited by many silicide compounds. Table 2 summarizes various silicide nanostructures synthesized. Up to now from the eight transition metals that have been reported for forming silicide NWs, four of them have more than one reported phase as shown in Table 2. For instance, there are six known iron silicide intermetallic compounds ( $\text{Fe}_3\text{Si}$ ,  $\text{Fe}_2\text{Si}$ ,  $\text{Fe}_5\text{Si}_3$ ,  $\text{FeSi}$ ,  $\alpha\text{-FeSi}_2$ ,  $\beta\text{-FeSi}_2$ ) only three of which are stable at room temperature [42].

IA	IIA	IIIB	IVB	VB	VIB	VIIIB	VIII	VIII	VIII	IB	IIB
H <sub>4</sub> Si											
Li <sub>15</sub> Si <sub>4</sub> Li <sub>2</sub> Si											
NaSi NaSi <sub>2</sub>	Mg <sub>2</sub> Si										
KS KS <sub>3</sub>	Ca <sub>2</sub> Si Ca <sub>5</sub> Si <sub>3</sub> CaSi CaSi <sub>2</sub>	Sc <sub>5</sub> Si <sub>3</sub> ScSi Sc <sub>2</sub> Si <sub>3</sub> Sc <sub>3</sub> Si <sub>5</sub>	Ti <sub>3</sub> Si <b>Ti<sub>6</sub>Si<sub>3</sub></b> Ti <sub>5</sub> Si <sub>4</sub> <b>TiSi</b> <b>TiSi<sub>2</sub></b>	V <sub>3</sub> Si V <sub>2</sub> Si V <sub>5</sub> Si <sub>3</sub> VSi <sub>2</sub>	Cr <sub>3</sub> Si Cr <sub>5</sub> Si <sub>3</sub> CrSi <b>CrSi<sub>2</sub></b>	Mn <sub>4</sub> Si Mn <sub>3</sub> Si Mn <sub>5</sub> Si <sub>2</sub> <i>Mn<sub>5</sub>Si<sub>3</sub></i> MnSi <b>MnSi<sub>2-x</sub></b>	Fe <sub>3</sub> Si <b>(Fe<sub>6</sub>Si<sub>3</sub>)</b> <b>FeSi</b> <b>FeSi<sub>2</sub></b>	<b>(Co<sub>3</sub>Si)</b> <b>Co<sub>2</sub>Si</b> <b>CoSi</b> Co <sub>2</sub> Si <sub>3</sub> CoSi <sub>2</sub>	<b>Ni<sub>3</sub>Si</b> <b>Ni<sub>2</sub>Si</b> <b>Ni<sub>31</sub>Si<sub>12</sub></b> <b>Ni<sub>3</sub>Si<sub>2</sub></b> <b>NiSi</b> <b>NiSi<sub>2</sub></b>	Cu <sub>3</sub> Si Cu <sub>15</sub> Si <sub>4</sub> Cu <sub>5</sub> Si	
RbSi RbSi <sub>6</sub>	Sr <sub>5</sub> Si <sub>3</sub> SrSi SrSi <sub>2</sub>	Y <sub>5</sub> Si <sub>3</sub> Y <sub>5</sub> Si <sub>4</sub> YSi Y <sub>3</sub> Si <sub>5</sub> Y <sub>2</sub> Si <sub>3</sub> YSi <sub>2</sub>	Zr <sub>3</sub> Si Zr <sub>2</sub> Si Zr <sub>5</sub> Si <sub>3</sub> Zr <sub>3</sub> Si <sub>2</sub> Zr <sub>6</sub> Si <sub>3</sub> ZrSi ZrSi <sub>2</sub>	Nb <sub>4</sub> Si Nb <sub>3</sub> Si Nb <sub>5</sub> Si <i>NbSi<sub>2</sub></i>	Mo <sub>3</sub> Si Mo <sub>5</sub> Si <sub>3</sub> Mo <sub>3</sub> Si <sub>2</sub> <i>MoSi<sub>2</sub></i>	Tc <sub>4</sub> Si Tc <sub>3</sub> Si Tc <sub>5</sub> Si <sub>3</sub> TcSi Tc <sub>4</sub> Si <sub>7</sub>	Ru <sub>2</sub> Si Ru <sub>5</sub> Si <sub>3</sub> Ru <sub>4</sub> Si <sub>3</sub> RuSi Ru <sub>2</sub> Si <sub>3</sub>	Rh <sub>2</sub> Si Rh <sub>5</sub> Si <sub>3</sub> Rh <sub>3</sub> Si <sub>2</sub> RhSi Rh <sub>4</sub> Si <sub>6</sub> Rh <sub>3</sub> Si <sub>4</sub>	Pd <sub>5</sub> Si Pd <sub>4</sub> Si Pd <sub>3</sub> Si <i>Pd<sub>2</sub>Si</i> PdSi		
CsSi CsSi <sub>3</sub>	Ba <sub>2</sub> Si Ba <sub>5</sub> Si <sub>3</sub> BaSi BaSi <sub>2</sub>	La <sub>5</sub> Si <sub>3</sub> La <sub>3</sub> Si <sub>2</sub> La <sub>5</sub> Si <sub>4</sub> LaSi LaSi <sub>2</sub>	Hf <sub>2</sub> Si Hf <sub>5</sub> Si <sub>3</sub> Hf <sub>3</sub> Si <sub>2</sub> Hf <sub>5</sub> Si <sub>4</sub> <i>HfSi</i> HfSi <sub>2</sub>	Ta <sub>3</sub> Si Ta <sub>2</sub> Si Ta <sub>5</sub> Si <sub>3</sub> <b>TaSi<sub>2</sub></b>	W <sub>3</sub> Si W <sub>5</sub> Si <sub>3</sub> <i>WSi<sub>2</sub></i>	Re <sub>3</sub> Si Re <sub>5</sub> Si <sub>3</sub> ReSi <i>ReSi<sub>1.75</sub></i>	OsSi OsSi <sub>2</sub> OsSi <sub>3</sub>	Ir <sub>3</sub> Si Ir <sub>2</sub> Si Ir <sub>3</sub> Si <sub>2</sub> IrSi IrSi <sub>3</sub>	Pt <sub>3</sub> Si Pt <sub>12</sub> Si <sub>5</sub> <i>Pt<sub>2</sub>Si</i> Pt <sub>6</sub> Si <sub>5</sub> <b>PtSi</b>		

**Table 2 Periodic table of the transition metal silicide phases [26]**

In such complicated materials systems careful control over synthesized phases can be quite difficult. In the last five years, several techniques have been developed for the synthesis of free-standing silicide NWs, which can be conveniently categorized into four groups:

- 1) Decomposition of silicon on metal thin films
- 2) Reaction of metals with silicon substrate
- 3) Simultaneous metal and silicon delivery
- 4) Silicidation of silicon (Si) NWs

## 1.2.1 Synthesis of silicide nanostructures

### a. Decomposition of silicon on metal thin films

One of the approaches for producing silicide nanostructure as reported in literature has been the delivery of one of the components of the aforementioned material ( $MSi_x$ ) in the form of vapour, liquid or solid to the other element as substrate. This approach can be advantageous as fewer gas phase species simplifies the experiments. Since silicon has a melting point of over 1400 °C it would be impractical to deliver the silicon as single element vapour. Instead the use of  $SiCl_4$  and  $SiH_4$  has been reported to have successfully been employed for the use of Silicide synthesis at temperatures ranging from 320-600 °C. A scheme for the delivery of Si using silane precursors was easily adopted from the wealth of reports detailing CVD synthesis of silicon NWs [44,45]. Interestingly, to date this strategy has only been reported for NWs of nickel silicides:  $NiSi_2$  [27],  $NiSi$  [28,29],  $Ni_2Si$  [30],  $Ni_3Si_2$  [29] and  $Ni_3Si$  [31] (all of the room temperature stable nickel silicide phases). Based on these reports we can conclude that the differences in the Ni content is associated with temperature and pressure, however, it could not be taken for granted that temperature is the only deciding factor in the nanowire growth though exact details of the experiments have not been disclosed yet. For example, it has been reported that at a temperature of 550 °C, Qi et al. have obtained [32]  $Ni_3Si_2$  phase nanowires while at a lower temperatures there are several reports of  $NiSi_2$  and  $NiSi$  which can be related to the temperature dependency of diffusion process. The other important factor which affects the synthesis process is the partial pressure of reacting gases on the growth of these nanowires. Kang et al. [33] have done a detailed investigation on the effect of the

introduction of  $H_2$ ,  $O_2$  and  $N_2$  on the growth. In Fig1.6a, the schematics of the growth process is shown. Primarily in all the synthesis processes of NiSi they have used an oxide barrier between the Ni layer and the silicon wafer so to prevent the diffusion of the Nickel into the silicon (Nickel is highly diffusive in silicon). Fig1.6b-d show the impact of these atmosphere conditions. They reported with  $H_2$  atmosphere they observed the deposition of only grains of  $NiSi_x$  and no nanowires, with  $N_2$  they had a mixed

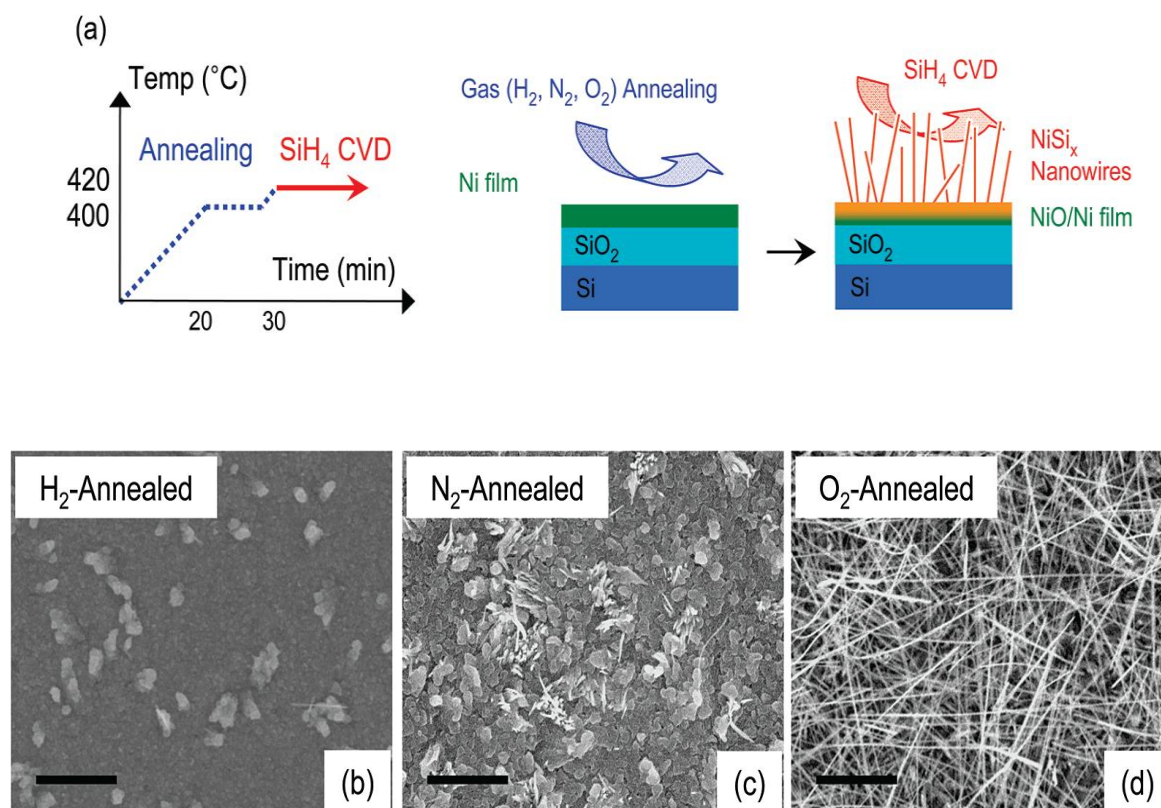


**Figure 2.6 (a) The schematics of the spontaneous nanowire growth in this study. (b-d) The representative SEM images of the reaction products on H<sub>2</sub>-, N<sub>2</sub>-, and O<sub>2</sub>-annealed samples, respectively. Scale bar 1um.**

production and with oxygen they successfully synthesized large amount of Ni<sub>2</sub>Si nanowires which is the cause of NiO<sub>x</sub> formation on the surface. Kang et al., proposed that

this oxide will give limited access for the diffusion of the Ni seeds underneath that ultimately results in the formation of nanostructures.

Even with reports dating back to 2004, little significant work has been done to uncover the mechanism behind this particular growth method. A possible reason that this strategy has been reported only for nickel silicides is the extremely fast diffusion of Ni in Si. Many transition metals can be used to catalyze Si NW growth via either the VLS mechanism or the vapour-solid-solid (VSS) mechanism. Ni itself is actually one of the earliest reported VLS catalysts for Si NW growth [34].

## **b. Reactions of metal sources with silicon substrates**

In this method, transition metal species can directly react with silicon substrates to make silicide NWs. While a variety of simple organometallic complexes are known to decompose to deliver metal [35], date only pure metal vapours and anhydrous metal halides have been used to yield free standing metal silicide NWs.

### **I. Metal vapour**

Chueh and co-workers initially reported the synthesis of short (0.2–2  $\mu\text{m}$ )  $\text{TaSi}_2$  NWs via annealing silicon substrates with  $\text{FeSi}_2$  thin films or  $\text{FeSi}_2$  nanodots on their surface in a tantalum (Ta) atmosphere [36]. It was believed that Si atoms segregate from either the  $\text{FeSi}_2$  thin film or nanodots to form a Si based nano particles. Ta atoms adsorb onto the surface of either the  $\text{FeSi}_2$  thin films or nanodots and react with Si diffusing through the substrate to form  $\text{TaSi}_2$  nanocrystals. Because of the high temperatures and



low pressures used, oriented growth of certain facets is favoured and one-dimensional growth is observed. As it is apparent in Fig1.7a-b the density of the products is very low. One of the reasons for that is likely to be the high melting point of tantalum (3017 °C) which would give low vapour pressure of this metal.

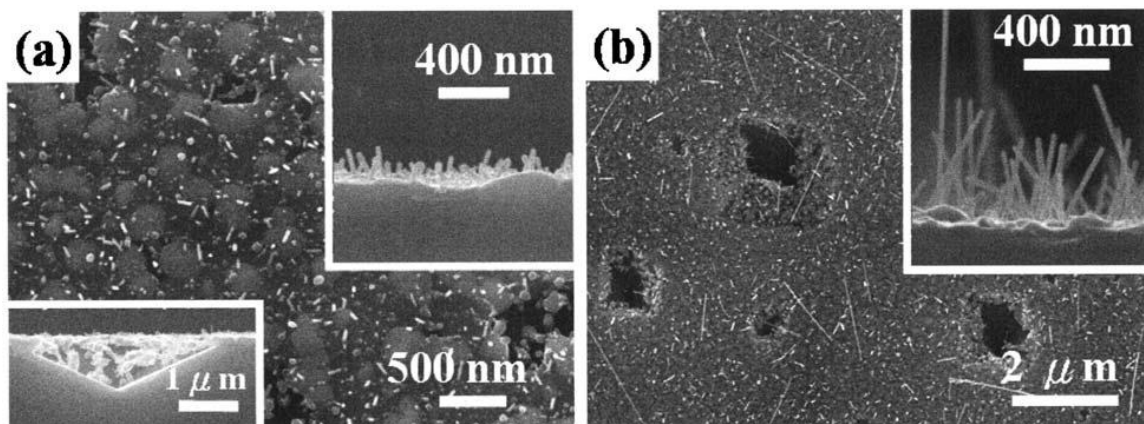


**Figure 2.7.** Top-view SEM image of nanowires, 950 °C, 16 h, a) FeSi<sub>2</sub> film on Si, the dark contrast regions correspond to the pinholes. Upper inset shows a side-view SEM image. The bottom inset shows side-view SEM image of a pinhole, b) FeSi<sub>2</sub> nanodots on Si. Upper inset shows a side-view SEM image.

The use of a different silicide film can increase the aspect ratio of generated NWs [37]; however, in all cases the metal impurity from the starting silicide thin film (or nanodots) is found in the final product, accounting for as much as 10% of the total elemental content. Other work reported by the same group provides more insight; annealing similar FeSi<sub>2</sub> substrates in the absence of Ta vapour but under higher temperature conditions produces silicon NWs. This result is not surprising considering the well-known use of Fe and its metal silicides as VLS or VSS catalysts for the growth of Si NWs; Fe was one of the first VLS catalysts reported [34].

## II. Metal halides

The application of anhydrous metal halides as the transition metal source for reaction with Si substrates has proven to be a general and popular method to grow silicide NWs. Ouyang and co-workers reported this technique as a facile way to produce FeSi nanowires using FeCl<sub>3</sub> [38]. Varadwaj et al. further used a two zone furnace to give better control of the metal halide vapour pressure. Typically, a halide precursor is vaporized in the upstream zone of a furnace, kept around 500 °C, and the substrate is held at 900 °C during the course of the reaction. Interestingly, by using substrates other than Si, metal rich phases can be favoured (Si powder or a Si substrate is still required for NW growth) [39]. Using this approach, NWs of FeSi [40], TiSi<sub>2</sub> [41], Ti<sub>5</sub>Si<sub>3</sub> [42], Fe<sub>5</sub>Si<sub>3</sub> [39], CoSi [43], Co<sub>2</sub>Si [43], CrSi<sub>2</sub> [44], and Fe<sub>11-x</sub>Co<sub>x</sub>Si [45] have been reported. As an example, Seo et al. [46] showed that using CoCl<sub>2</sub> as the Co precursor and using silicon or a sapphire substrate near silicon, they can achieve different compositions of CoSi<sub>x</sub>. According to their work, when they had silicon as substrate the proposed reaction is:



Same reaction has been proposed for other silicides that have used a halide and silicon as substrate[38,39]. Also in this report they have investigated the use of sapphire as substrate. The configuration of their experiment is illustrated in Fig1.8a and b. The substrate and the silicon wafer was positioned in the high temperature zone and the CoCl<sub>2</sub> was set at the upstream at a lower temperature.

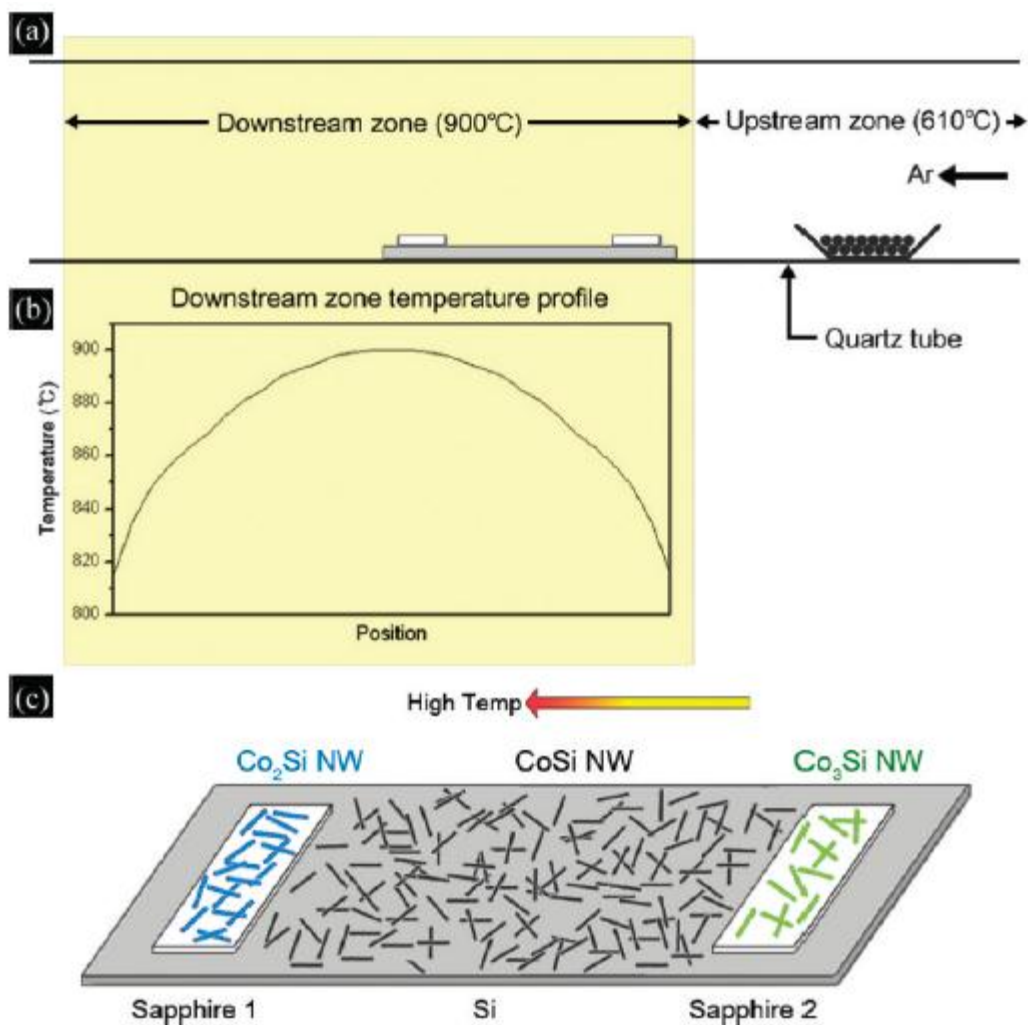


Figure 2.8. Experimental setup. (a) Horizontal tube furnace with two independently controlled heating zones. (b) Temperature profile indicates that the center of the downstream zone is at 900 °C, and the substrates are at 820-890 °C. (c) Tilted view illustration of the substrate placement in panel a. A rectangular Si wafer (50mm-150 mm) kept at the downstream zone played a role of Si source for NW synthesis.  $\text{Co}_2\text{Si}$  NWs are grown on the sapphire 1 substrate,  $\text{CoSi}$  NWs on the Si, and  $\text{Co}_3\text{Si}$  NWs on the sapphire 2.

According to their results the following reactions have been proposed:



It was explained that the reactions differed according to the distance of substrate and silicon. Similar reactions have been proposed with rather similar configuration for other silicides [59-61].

Although no convincing mechanism has been reported, vapour-solid (VS) mechanisms are usually proposed based largely on the delicate dependence of halide supersaturation on the resultant silicide morphology and phase. At lower pressures, the halides become more volatile and metal rich phases are preferred. Metal chlorides are well known to react with Si to produce  $\text{SiCl}_4$ ,  $\text{MSix}$ , and/or  $\text{Cl}_2$ .  $\text{SiCl}_4$  is likely providing vapour-phase Si that could decompose to form elemental silicon or silicide, releasing more  $\text{Cl}_2$  into the vapour phase.  $\text{SiCl}_4$  is widely used to grow silicon NWs at such high temperatures.

### **c. Simultaneous metal and silicon delivery**

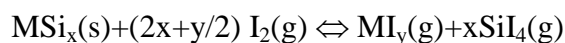
Simultaneous delivery of silicon and transition metal source material to a substrate to grow metal silicide NWs has been achieved using two different techniques: chemical vapour transport (CVT) and chemical vapour deposition (CVD).

#### **I. Chemical vapour transport (CVT)**

CVT, a classical crystal growth method, takes advantage of the reversible thermodynamic reaction between two chemical species, a source material and a transport agent, to *in situ* produce gas phase precursors. The intermediates provide the elements needed to synthesize the desired phase, as shown in. This technique has been widely used to synthesize single crystals of many of the transition metal silicides [47]. However, one-

dimensional NW growth may be obtained by altering the process for kinetically-favoured growth of 1D morphologies.

The synthesis of three distinct single crystalline silicide NW phases via continuous-flow CVT using iodine (I<sub>2</sub>) as the transport agent have been demonstrated. In each case, growth occurred on Si/SiO<sub>2</sub> substrates, sometimes requiring a dilute metal salt solution of Ni(NO<sub>3</sub>)<sub>2</sub> on the surface. Hexagonally faceted CrSi<sub>2</sub> NWs with lengths up to a few hundred microns were synthesized using powdered CrSi<sub>2</sub> as the source material. NWs of the d-Ni<sub>2</sub>Si [48] and b-Ni<sub>3</sub>Si [49] phases were also synthesized using Ni<sub>2</sub>Si and TiSi<sub>2</sub> as source materials, respectively. For both CrSi<sub>2</sub> and d-Ni<sub>2</sub>Si, the product stoichiometry was identical to the stoichiometry present in the source material. Due to the fact that NiSi<sub>x</sub> have high melting point it would be very impractical to raise the temperature to their melting point. Instead the use of I<sub>2</sub> which would react with the silicide in the equation below would be favourable (Fig1.9) :



Although the exact growth mechanism has not been determined for CVT grown silicide NWs, the lack of a visible catalyst tip combined with the necessity of the metal salt solution has been used to rule out VLS-type growth and typically vapour solid or metal-assisted NW growth.

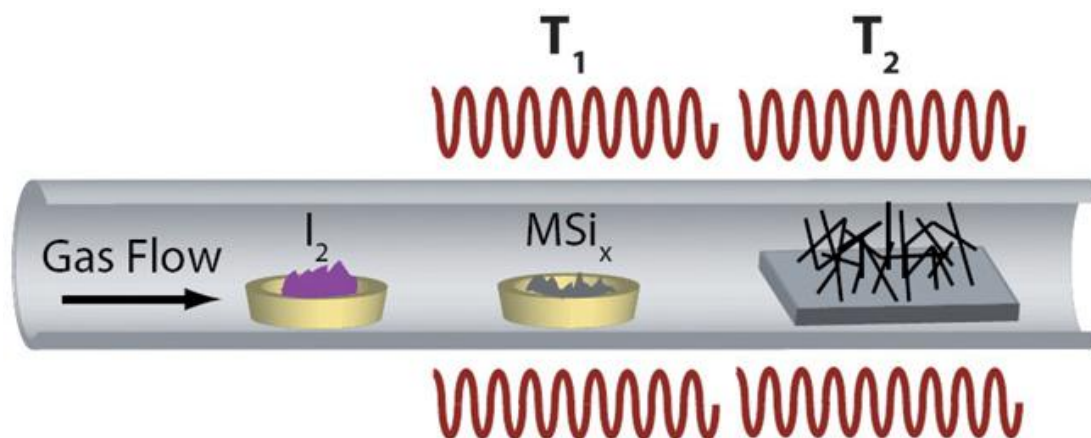


**Figure 2.9** Synthesis of metal silicide NWs using chemical vapour transport (CVT). Silicides undergo reversible reaction with  $I_2$  at  $T_1$  to form in situ gas phase products. At  $T_2$  gas phase components undergo the reverse reaction to form silicide NWs.

## II. Chemical vapour deposition (CVD)

Usually single source precursors are used in the CVD method for producing silicide nanowires. To date, the use of single source precursors (SSP) of inorganic complexes containing the transition metal and silicon atoms necessary for silicide formation has been shown to be one of the most successful and versatile transition metal silicide NW synthesis techniques. SSPs have been used in MOCVD to grow transition metal silicide thin films. Compared with conventional multisource metal organic CVD, the SSP approach allows simpler and safer experimental setups due to the elimination of highly hazardous liquid precursors ( $Fe(CO)_5$  typically for Fe and  $SiCl_4$  for Si), easier and precise control over stoichiometry, and growth of higher quality materials, i.e. FeSi

## CVD Using Single Source Precursors

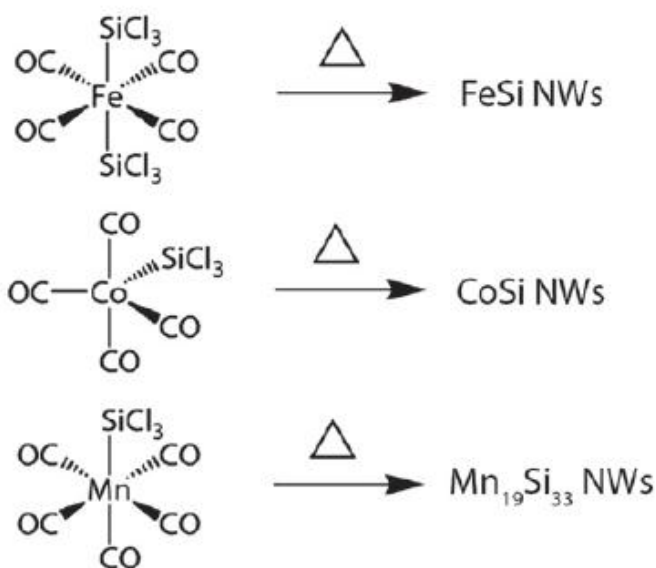
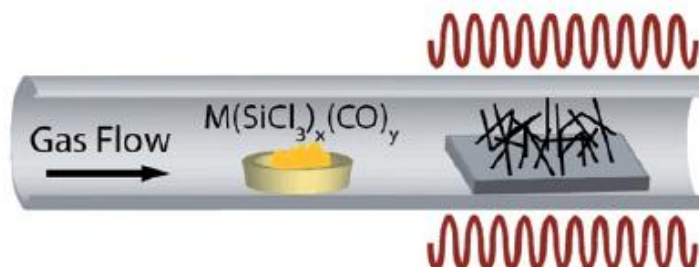
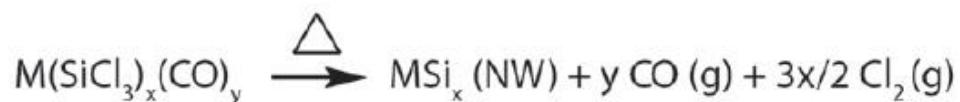


**Figure 2.10** Synthesis of metal silicide NWs using chemical vapour deposition (CVD) of single source precursors (SSP). Each SSP pyrolyzes to deliver metal silicide material to the growth substrate.

and CoSi thin films have been deposited by the pyrolysis of  $\text{Fe}(\text{CO})_4(\text{SiCl}_3)_2$  [50] and  $\text{Co}(\text{CO})_4\text{SiCl}_3$  [51]. By selecting simple inorganic molecules containing metal and silicon that vaporize and decompose through well-known pathways, precise control of the product stoichiometry and reproducible growth of NWs is possible (Fig1.10). The production of these macro molecules have been discussed in these reports. Other

molecules that have been produced that subsequently were used for silicide materials are  $\text{MnSi}_{2-x}(\text{MnSi}_{1.8})$  with the substrate being a silicon wafer covered by a cobalt film which was applied for the synthesis of CoSi NWs,  $(\text{MnSi}_{1.8})$  NWs using  $\text{Mn}(\text{CO})_5\text{SiCl}_3$  and also there has been report of the use of mixture of  $\text{trans-Fe}(\text{CO})_4(\text{SiCl}_3)_2$  and  $\text{Co}(\text{CO})_4\text{SiCl}_3$  as single source precursor which is a liquid solution. This solution can be conveniently evaporated for vapour phase delivery resulting in the synthesis of  $\text{Fe}_{1-x}\text{Co}_x\text{Si}$  alloy NWs.

#### **d. Silicidation of silicon nanowires**

Lieber and co-workers firstly reported the growth of transition metal silicide NWs by silicidation of silicon nanowires (Fig1.10a,b). A Si NW backbone, formed using a standard Au nanoparticle mediated VLS process, was covered with a thermally evaporated Ni thin film. Subsequent annealing in forming gas produced single-crystalline NiSi NWs via solid state reaction. Furthermore, epitaxial heterojunctions of NiSi and Si were demonstrated allowing the integration of high performance nanowire transistors beyond the lithographic limit. The main challenges in silicide NW formation, material delivery and 1-D anisotropic growth, were overcome independently using this methodology. This work was easily extended to other metals such as Fe to form FeSi, a- $\text{FeSi}_2$ , and b- $\text{FeSi}_2$  NWs. and platinum (Pt) resulting in PtSi NWs. However, the nanowires produced in these latter cases were not single crystals. The stoichiometry of silicided NWs could likely be controlled by carefully managing the concentration of evaporated metal; however, certain phases will probably be unobtainable through this technique due to the kinetics factor of the diffusion process, while they are obtained in



thin film and bulk diffusion couples. Such diffusion couples between metals and silicon have been widely studied [52].

Although there has many reports of experiments on the performance of nanowires synthesized with this method, it remains a way to understand different aspects of silicidation instead of a technique for mass production of NWs due to complicated nature of the synthesis process.

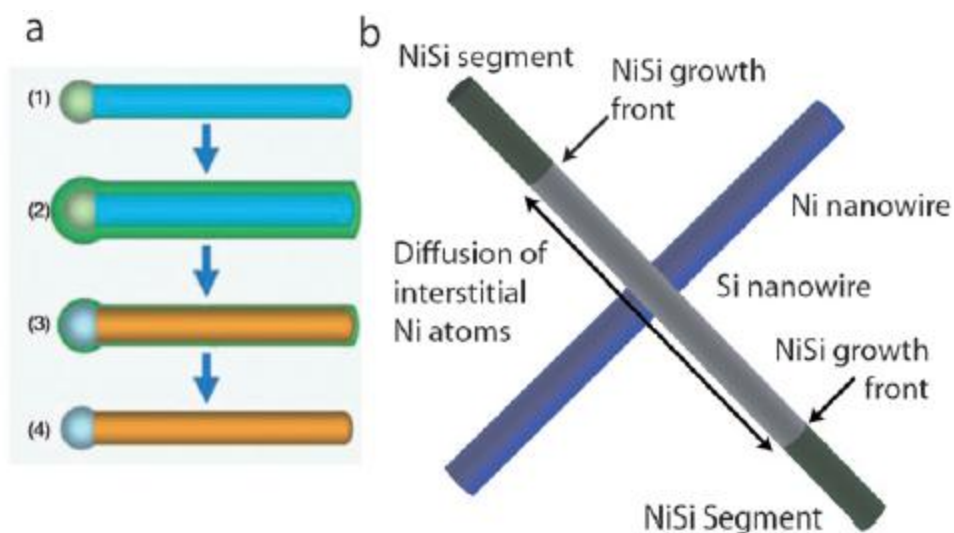


**Figure 2.11** Preparation of NiSi NWs by silicidation. a1) Si NWs (blue) are synthesized via VLS and a2) coated with Ni metal (green), a3) reacted at 550 °C to form NiSi nanowires (orange). a4) Extra Ni metal is etched away leaving single crystalline NiSi NWs.62 b) Preparation of NiSi NWs by point contact silicidation to form NiSi–Si NW heterostructures.

### 1.3. Applications

Transition metal silicides have been extensively used in a large number of applications owing to their diverse physical properties, such as high melting points, excellent chemical stability, and compatibility with silicon processing technology, which

make them good candidate materials for use in electronics, thermoelectrics, and photovoltaics. Metal silicide nanowires share these positive characteristics and their size may allow them to be potential candidates to improve nanoscale versions of these devices as well as playing new roles, such as field emission sources nanoelectronics, thermoelectrics, solar energy conversion and spintronics. In the following section we will briefly review nanoelectronics and nanoscale field emission applications and their concepts utilizing silicide NWs.

## **Nanoelectronics**

Because of the ubiquity of metal silicides as interconnects and contact electrodes in modern microelectronics [53], silicide NWs are expected to serve a similar role in nanoelectronic devices. Their low resistivity and compatibility with silicon make them excellent candidates to continue in this role. Notably, ultra long  $\text{Ni}_2\text{Si}$  NWs were made having an extremely low resistivity of  $21 \mu\Omega\cdot\text{cm}$  and were capable of supporting remarkably high failure current densities  $>10^8 \text{ A/cm}^2$  (Fig1.10) [54]. The difficulty of selective nanostructure placement for devices serves as a strong barrier against the use of randomly oriented free standing NWs.

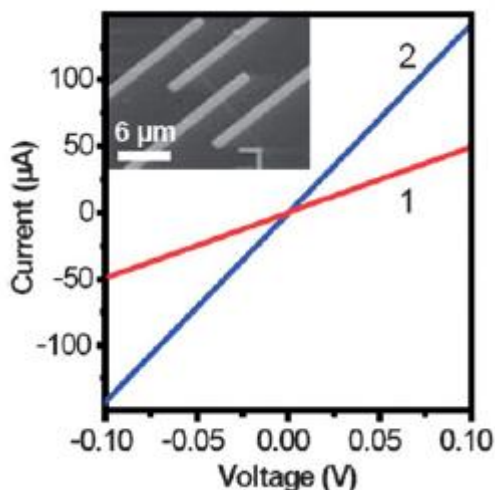


Figure 2.12 Two-probe (1) and four-probe (2) electrical transport for single  $\text{Ni}_2\text{Si}$  NWs

### Nanoscale field emitters

Another commonly discussed application for metal silicide NWs is their use as nanoscale field emitters. Field emission occurs when an electric field between a metallic surface and a ground electrode allows electrons to overcome the work function potential that binds them on the surface of the emitter. Field emission devices are useful in wide ranging applications such as flat panel displays, microwave generation devices, and high powered vacuum microelectronic devices. Since the late 1990s there has been much interest in developing 1-D nanomaterials for field emission due to the enhancement of electric field at the high curvature tips. Attributing to their low resistivity, work function, high melting points, high aspect ratios, and well known compatibility with silicon-based microelectronics, transition metal silicide nanowires have been considered good candidates for future field emission devices.

## Li-Ion Batteries

Lithium Ion Batteries are energy storage systems that convert chemical energy stored in electrodes to electrical energy via electrochemical reduction-oxidation (redox) reactions. Due to the rapid increase in the use of portable computers, mobile phones, video cameras, electric vehicles, etc., there is an increasing demand for rechargeable batteries with larger capacity, smaller size, lighter weight and lower price. Silicide nanomaterials have been one of the possible candidates that can be used as anode materials to improve the performance of Lithium Ion Batteries.

The most important reason for the use of silicon based materials is due to their highest theoretical capacity of approximately  $4200 \text{ mahg}^{-1}$  for lithium insertion at fully lithiated phase ( $\text{Li}_{22}\text{Si}_5$  or  $\text{Li}_{4.4}\text{Si}$ ) among known substances [55,54]. Silicide material although reduce that capacity somewhat compared to the use of only silicon nanomaterial, nonetheless exhibit higher stability. One of the silicide materials that a number of previous reports have mentioned for the anode electrode in Lithium Ion Batteries is  $\text{NiSi}_x$ . Figure 1.13a,b shows an SEM image of  $\text{Ni}_3\text{Si}$  nanowalls synthesized using chemical vapour deposition by H. Zhang et. al. [56]. The performance of the battery cell tested by this group as it is apparent in Fig1.13c, shows a good stability for 20 cycles.

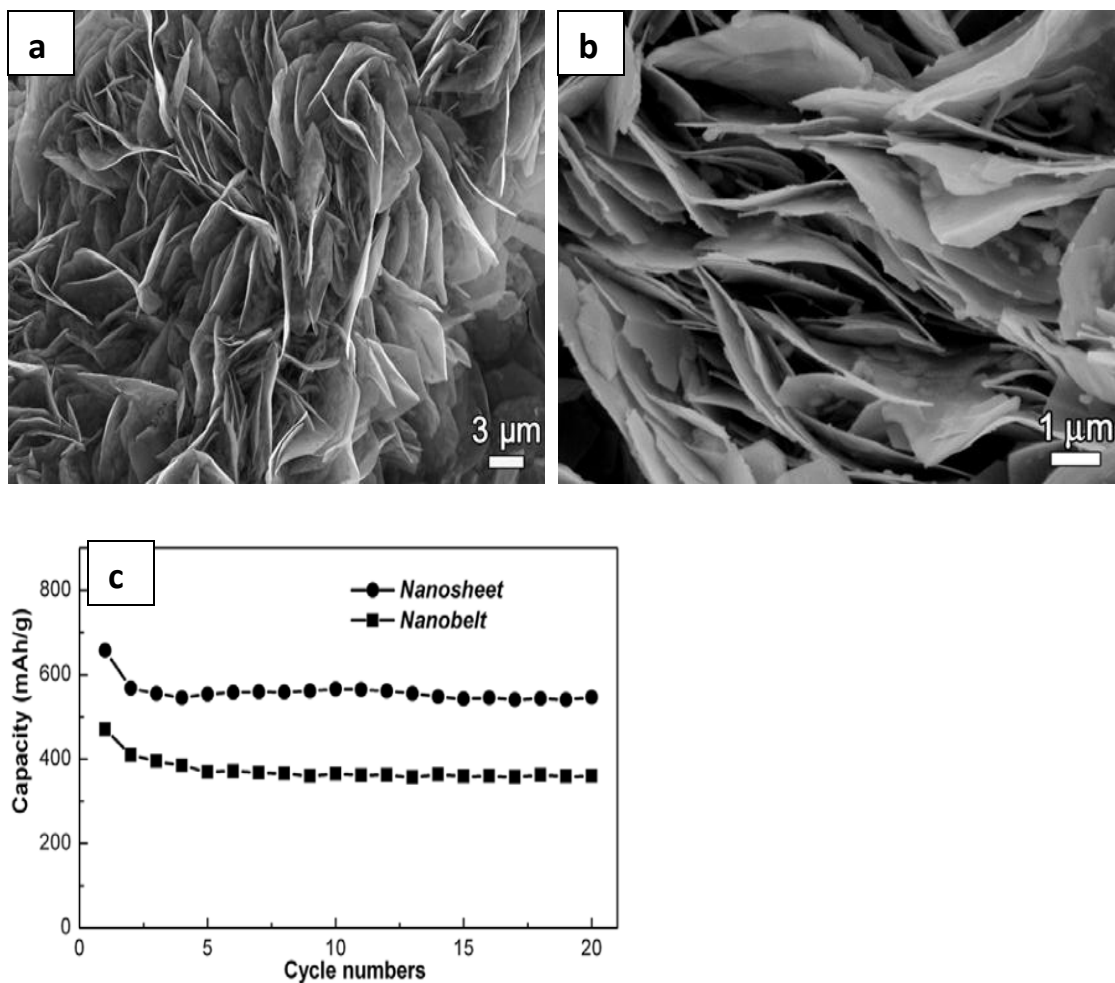


Figure 2.13 (a), (b) Top-view SEM images of the Ni silicide nanosheets (c) Electrochemical performance of the Ni silicide nanosheets (comprising  $\text{Ni}_3\text{Si}$  and  $\text{Ni}_{31}\text{Si}_{12}$ ) grown on a Ni foil substrate and of the Ni silicide nanobelts ( $\text{Ni}_3\text{Si}$ ) grown on a Ni foam substrate.

## 1.4. Conclusion

In Summary, nanomaterials have been synthesized through various methods for different applications. Silicide materials have proven to be great candidates for a variety of different applications. The number of synthesis method allows further researchers to find the most practical and feasible strategy for developing the desired use. Studies on the growth of the nanowires  $\text{NiSi}_x$  and  $\text{CoSi}_x$  have been of particular interest to us for their

unique properties as anode materials in Lithium Ion Batteries. The few reports of the applying these materials for this purpose which has led us to further improve and investigate this area.

### **1.5. Outline and objectives of this thesis**

The objectives of this thesis are to synthesize nanostructures of  $\text{NiSi}_x$  and  $\text{CoSi}_x$  on various substrates such as Silicon wafer, carbon paper and Ni foam using CVD method. This thesis includes 5 chapters ( two introductory chapters and two article chapters and one final chapter for conclusion and future work) which is in the format of “integrated article” . The thesis is submitted in accordance to the Thesis Regulations Guide of Society of Graduate and Postdoctoral Studies (SGPS) . The Thesis content consists of :

**Chapter 1** gives an introduction on nanomaterials and their growth mechanism. Silicide nanomaterials are focused and their applications and synthesis method are discussed based on the reports given on this field.

**Chapter 2** Explains the experimental procedure carried out in the experiments. The devices used for this purpose are mentioned. Characterization and analysis techniques employed have been stated and a brief description of their mechanism has been given.

**Chapter 3** Synthesis process of NiSix on carbon paper, silicon wafer and Ni foam using Chemical Vapour Deposition method is mentioned and the parameter effects and growth mechanism are discussed.

**Chapter 4** Synthesis process of CoSix using CVD method on carbon paper were stated. The experiments were optimized at two different pressure levels and characterization of the products was performed for each. Parameter effects on the morphology and structure of the nanowires were investigated .

**Chapter 5** summarizes the results and contributions of the thesis work. In addition, the author gives some personal opinions and suggestions for future work.

## References

1. **X. Wang, M. Waje and Y. Yan.** 2005, *Electrochemical and solid state letters*, pp. 8,1,A42.
2. **S. Yao, J. Xu , Y. Wang, X. Chen , Y. Xu and S. Hu.** 2006, *Analytica chemical acta*, pp. 557,1-2,78.
3. **T. Kato, Y. Tanaka, T. Hirata, S. Kumamoto and K. Miyazaki.** 1997, *Journal of Materials science letters*, pp. 16,21,1771.
4. **C. Shao, H. Guan, Y. Liu, X. Li and X. Yang.** 2004, *Journal of solid state chemistry*, pp. 177,2628.
5. **Iijima, S.** 2001, *Nature* 1991, pp. 354,56.
6. **H. Wang, C. T. Yip, K. Y. Cheung, A. B. Djuricic, M. H. Xie, Y. H. Leung and W. K. Chan.** 2006, *Applied physics letters*, pp. 89,2,23508.
7. **R. Hauschild, H. Lange, H. Priller, C. Klinshrin, R. Kling, A. Waag, H. J. Fan, M. Zacharias and H. Kalt.** 2006, *Physica status solidi B.*, pp. 243,4 ,853.
8. **M. Bystrzejewski, A. Huczko, P. Byszewski, M. Doman´ska, M. H. Ru´mmeli, T. Gemming, and H. Lange.** s.l. : Taylor and Francis, 2009. 17,298-307.
9. **N. Braidya a, M.A. El Khakani a, G.A. Botton.** s.l. : *Chemical Physics Letter*, 2002. 354,88-92.
10. **P. Castrucci, M. Scarselli , M. D Crescenzi , M. Diociaiuti , P S. Chaudhari.** s.l. : *Thin Solid Film*, 2006. 508, 226-307.
11. **H. J. Fan, W. Lee, R. Hauschild, M. Alexe, G. L. Rhun, R. Scholz, A. Dadgar, K. Nielsch, H. Kalt, A. Krost, M. Zacharias and U. Gosele.** 2006, *small*, pp. 4,561.
12. **Z. Wang, Z. Pan.** 2002, *advanced materials*, pp. 14,1029.
13. **C. N. R. Rao, A. Muller, A. K. Cheetham.** s.l. : Wiley-VCH, 2004, Vol. Vol.1.
14. *Effect of RuO<sub>2</sub> in the shape selectivity of submicron-sized SnO<sub>2</sub> structures.* **N. S. Ramgir, I. S. Mulla and K. P. Vijayamohan.** 109, 25, 12297, *journal of physical chemistry B* : s.n., 2005.
15. **H. Park, R. Beresford, R. Ha, H.J. Choi , H. Shin and J. Xu.** s.l. : *Nanotechnology* , 2005. 23 245201.
16. **Y. Yan, Y. Zhang, H. Zeng, J. Zhang, X. Cao and L. Zhang.** 18, 17], s.l. : *Nanotechnology*, 2007.



16. **N. +G. Ma, J. Lang and D. H. L. Nq.** 65,14,2167, s.l. : composite science and technology , 2005.
- 17 **Wu, K. W. Chang and J. J.** 20,12,3397, s.l. : journal of material research, 2005.
18. **N. Wang, K.K. Fung, S. Wang and S. Yang.** 233,1-2,226, s.l. : Journal of crystal growth, 2001.
19. **Z. Li, J. Baca and J. Wu.** 254,2,633, s.l. : Applied surface science, 2007.
20. **C. Tang, Y. Bando and T. Sato.** 106,30,7449, s.l. : Journal of physical Chemistry B, 2002.
21. **H.F. Yan, Y.J. Xing, Q.L. hang, D.P. Yu, Y.P. Wang, J. Xu, Z.H. Xi and S. Q. Feng.** 323,224, s.l. : Chemical Physics letters, 2000.
22. **C. Pfeleiderer, D. Reznik, L. Pintschovius, H. von Lohneysen, M. Garst and A. Rosch.** 427,227-231, s.l. : Nature , 2004.
23. **J. Derrien, J. Chevrier, V. Lethanh and J. E. Mahan.** 1992, appl. surf sci., pp. 56-58, 382-393.
24. **D. Leong, M. Harry, K. J. Reeson and K. P. Homewood.** 1997, nature, pp. 387, 686-688.
25. **Mahan, M. C. Bost and J. E.** 1988, appl. phys., pp. 63, 839-844.
26. **Andrew L. Schmitt, Jeremy M. Higgins, Jeannine R. Szczech and Song Jin.** s.l. : Journal of materials chemistry, 2009, Vol. 20. 2,197-400.
27. **X. Q. Yan, H. J. Yuan, J. X. Wang, D. F. Liu, Z. P. Zhou, Y. Gao,L. Song, L. F. Liu, W. Y. Zhou, G. Wang and S. S. Xie.,** 2004, Appl physics, pp. 76,1853-1856.
28. **Anderson, J. Kim and W. A.** 2005, thin solid film, pp. 483,60-65.
29. **C.-J. Kim, K. Kang, Y.-S. Woo, K.-G. Ryu, H. Moon, J.-M. Kim, D.-S. Zang and M.-H. Jo.** 2007, adv. mater, pp. 19,3637-3642.
30. **Z. Liu, H. Zhang, L. Wang and D. Yang.,** 2009, Nanotechnology, pp. 19,375602.
31. **J. Kim, E.-S. Lee, C.-S. Han, Y. Kang, D. Kim and W. A. Anderson.** 2008, Microelectron. Eng, pp. 1709-1712.
32. *CoO/NiSix core-shell nanowire arrays as lithium-ion anodes with high rate capabilities.* **Y. Qi, Ning Du, Hui Zhang,Xing Fan, Yang Yang and Deren Yang.** 2011, Nannoscale , pp. 4,991.
33. **K. Kang, S.-K. Kim, C.-J. Kim and M.-H. Jo.** s.l. : Nano Lett. , 2008. 8, 431-436.
34. **R. S. Wagner, W. C. Ellis, Trans. Am. Inst. Min.** 1965, metall. Pet. Eng, pp. 233, 1053-1064.

35. **A. N. Gleizes.** 2000, Chem. Vap. Deposition , pp. 6, 155–173.
36. **Y. L. Chueh, L. J. Chou, S. L. Cheng, L. J. Chen, C. J. Tsai, C. M. Hsu and S. C. Kung.,** 2005, appl. phys. lett., pp. 87, 223113.
37. **Y.-L. Chueh, M.-T. Ko, L.-J. Chou, L.-J. Chen, C.-S. Wu and C.-D. Chen.** 2006, Nano Lett., 2006, , pp. 6, 1637–1644.
38. **L. Ouyang, E. S. Thrall, M. M. Deshmukh and H. Park.** 2006, adv. mater, pp. 18,1437-1440.
39. **K. S. K. Varadwaj, K. Seo, J. In, P. Mohanty, J. Park and B. Kim.** 2007, j. am. chem soc., pp. 129, 8594-8599.
40. **H.-K. Lin, Y.-F. Tzeng, C.-H. Wang, N.-H. Tai, I. N. Lin, C.-Y. Lee and H.-T. Chiu.** 2008, Chem. Mater., pp. 20, 2429–2431.
41. **B. Xiang, Q. X. Wang, Z. Wang, X. Z. Zhang, L. Q. Liu, J. Xu and D. P. Yu.** 2005, appl. phys. lett, pp. 86,243103.
42. **H.-K. Lin, Y.-F. Tzeng, C.-H. Wang, N.-H. Tai, I. N. Lin, C.-Y. Lee and H.-T. Chiu.** 2008, chem matter, pp. 20,2429-2431.
43. **K. Seo, K. S. K. Varadwaj, P. Mohanty, S. Lee, Y. Jo, M.-H. Jung, J. Kim and B. Kim.** 2007, nano lett, pp. 7,1240-1245.
44. **K. Seo, K. S. K. Varadwaj, D. Cha, J. In, J. Kim, J. Park and B. Kim.** 2007 , J. Phys. Chem. C, pp. 111, 9072–9076.
45. **J. In, K. S. K. Varadwaj, K. Seo, S. Lee, Y. Jo, M.-H. Jung, J. Kim and B. Kim.** 2008, j. phys. Chem. c, pp. 112, 4748-4752.
46. **K. Seo, K. S. K. Varadwaj, D. Cha, J. In, J. Kim, J. Park and B. Kim.** s.l. : J. physics Chem. C, 2007. 111, 9072–9076.
47. **Koukouss, J. J. Nickl and J. D.** 1971, j. less common met., pp. 23,73.
48. **Y. Song, A. L. Schmitt and S. Jin.** 2007, nano lett., pp. 7,965-969.
49. **Jin, Y. Song and S.** 2007, appl. phys lett, pp. 90,173122.
50. **Colquhoun, B. J. Aylett and H. M.** 1977, j chem soc.,dalton trans., pp. 2058–2061.
51. **I. Novak, W. Huang, L. Luo, H. H. Huang, H. G. Ang and C. E. Zybilla.** 1977, organmetallics, pp. 16, 1567–1572.
52. **F. E. Rohrer, H. Lind, L. Eriksson, A. K. Larsson and S. Lidin,Z. Kristallogr.** 2000. 215,650-660.
53. **Maszara, W. P.** s.l. : J. Electrochem. Soc. , 2005. 152,G550–G555.

54. **Y. Song, A. L. Schmitt and S. Jin.** s.l. : Nano lett., 2007. 7,965-969.
55. **Okamoto, H.** 1990, Journal of Phase Equilibria, pp. 11(3) 306-312.
56. **C Tsai, C Y Wang, J Tang, M H Hung, K L. Wang , and L J Chen.** 2011, J. ACS Nano, pp. 9552-9558.

## Chapter 3 Experimental and Characterization Techniques

### 2.1. Chemical Vapor Deposition Synthesis Methods

Metal silicide nanostructures including  $\text{NiSi}_x$  and  $\text{CoSi}_x$  were synthesized on various substrates such as carbon paper and silicon wafer using a chemical vapor deposition method. For each metal silicide deposited on a specific substrate, the growth conditions were studied to obtain the optimum growth parameters for the high density synthesis of metal silicide nanostructures.

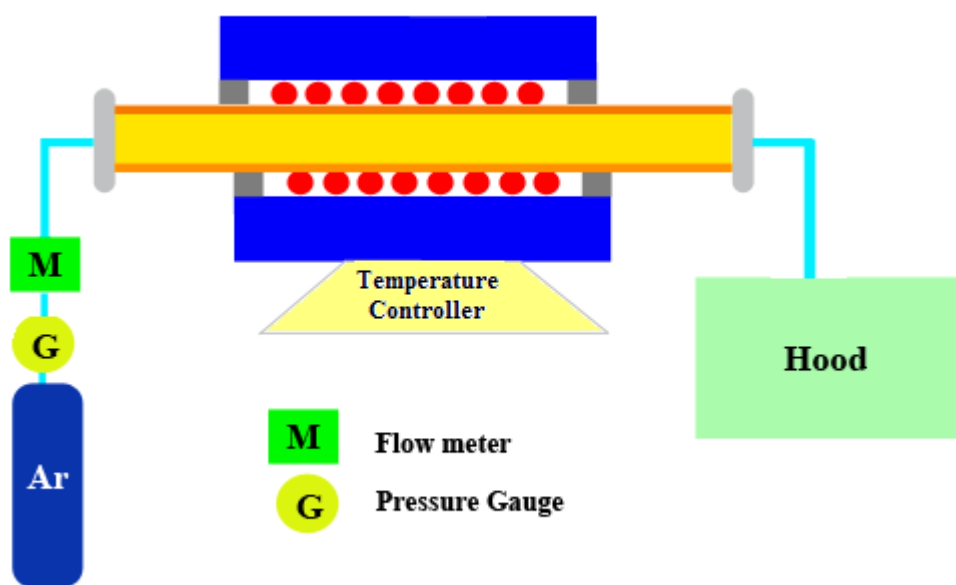


Figure 3.1 Schematic diagram of CVD method used for the synthesis of  $\text{NiSi}$  nanostructures.

#### 2.1.1. $\text{NiSi}_x$ Nanostructures

$\text{NiSi}_x$  nanowires were synthesized on carbon paper, silicon wafer, Ni foam substrates using a single zone chemical vapour deposition method in a horizontal quartz

tube furnace (LINDBERG/BLUE, Mini-Mite Tube Furnace, Model: TF55035A) system.

Fig2.1 shows a schematic diagram of the CVD process.

### Carbon Paper and Silicon Substrate

$\text{NiSi}_x$  nanostructures were synthesized on carbon paper and silicon wafer in the absence of any external catalysts. In this process carbon paper and silicon wafer the substrates were cleaned with ethanol for 10 min.  $\text{NiCl}_2 \cdot 6\text{H}_2\text{O}$  (Aldrich) and Si Powder (Aldrich, 99%) were used as the Ni and Si source respectively.

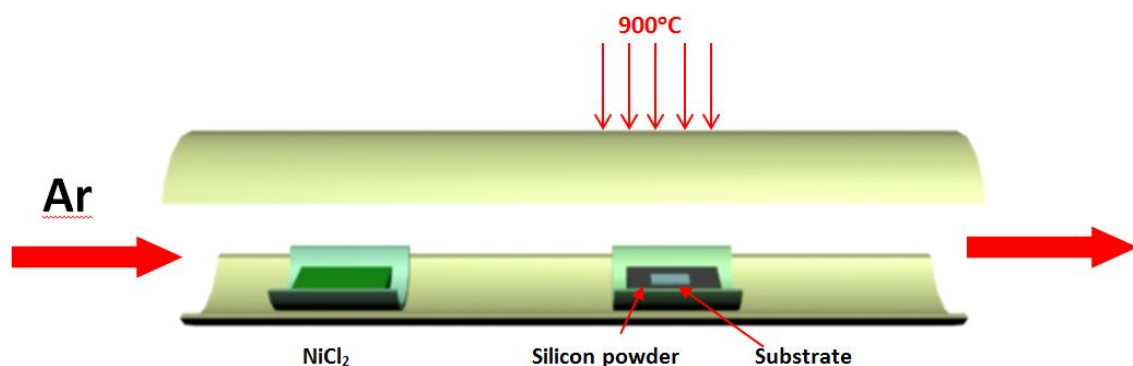


**Figure 3.2 Schematic diagram showing the setup of substrate and the sources in Quartz tube of CVD process for the synthesis of  $\text{NiSi}_x$  nanowires**

The substrate and source material were put in a quartz tube and mounted on the horizontal electrical furnace. As shown in Fig2.2, the substrates were placed the center of the heating region over the silicon powder at a temperature of 900 °C and the Ni source powder was placed at the edge of the furnace (low temperature region) where the temperature was between 200 °C-300 °C. High purity Ar (99.999%) was introduced into the system to purge the system from oxygen. The temperature was increased from room temperature to 900 °C at a heating rate of 18 °C /min and it was kept at this temperature

for 2 h. Ar flow of 200 sccm was maintained in the CVD chamber during the experiment as a carrier gas. After the furnace was cooled down to room temperature, a black layer was deposited on the substrates.

Various experiments were carried out to optimize the growth parameters including temperature, heating rate, time, gas composition,  $\text{NiCl}_2$  and Silicon source amount. The effect of these parameters was studied on the morphology of the nanostructure synthesized on the substrates.

### **Ni Foam Substrates:**

To synthesize  $\text{NiSi}_x$  nanostructures on Ni foam, these substrates were first treated with 2 mol of HCl acid (37%) for 5min and subsequently ethanol for 5 min.  $\text{NiSi}_x$  nanostructures were synthesized on Ni foam using a similar CVD method mentioned in the previous section.  $\text{NiCl}_2$  and silicon powder were used as the source materials. The temperature of the furnace was kept around 900 °C and the  $\text{NiCl}_2$  was positioned at the low temperature region of 600 °C.

Effect of various growth parameters was studied on the growth of  $\text{NiSi}_x$  nanostructures deposited on Ni foam. However unlike the nanostructures synthesized on carbon paper and silicon wafer, experimental results indicated that the composition of the carrier gas (addition of  $\text{H}_2$  to the carrier gas) also plays an important role on the morphology of nanostructures deposited on Ni foam.

### **2.1.2. CoSi Nanostructures**

CoSi nanowires were synthesized on carbon paper using chemical vapour deposition method (CVD) under different working pressures: 1) Atmospheric pressure and 2) Low pressure. In both studies  $\text{CoCl}_2 \cdot 6\text{H}_2\text{O}$  was used as Co source and due to their lower melting point, the Co sources were positioned in a lower temperature region at the upstream of the quartz tube (Fig2.3). Si powder (Aldrich, 99%) was used as the Si source. The Si powder along with carbon paper as the substrate was placed at the center of the heating zone (high temperature region) as seen in Fig2.3.

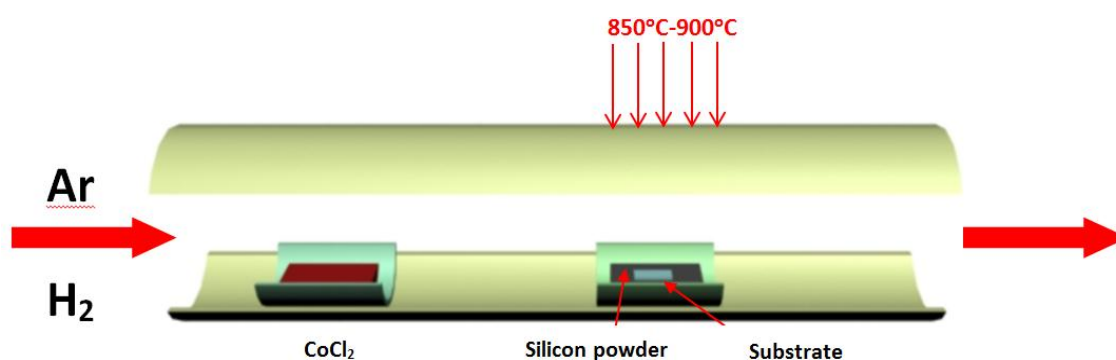


**Figure 3.3 Schematic diagram showing the setup of substrate and the sources in Quartz tube of CVD process for the synthesis of CoSi nanowires.**

Different parameters were investigated in order to optimize the growth conditions including temperature, time, configuration of the silicon and the substrate as well as heating rate. The optimum conditions for the growth of the nanostructures were found in both low pressure and atmospheric pressure. For low pressure experiments, the base pressure of experiment was 1 mbar and the working pressure, with a flow of Ar (99.999%) as carrier gas, was maintained at 10 mbar. The temperature of the furnace was set at 900 °C for 1h with a heating rate of 20 °C/min. For atmospheric pressure the temperature at the center of the heating zone was kept at 850 °C while  $\text{CoCl}_2$  was placed at a temperature zone of 550 °C.

## 2.2. Characterization Methods

The morphology and structure of nanomaterial deposited on the substrate were analyzed using a variety of analytical methods.

### 2.2.1. Scanning Electron Microscope (SEM)

Scanning electron microscope (SEM) is type of electron microscope to obtain different information from nanomaterials. The SEM uses a focused beam of high-energy electrons to generate a variety of signals at the surface of solid specimens. The signals that derive from electron-sample interactions reveal information about the sample including external morphology (texture), chemical composition, and crystalline structure and orientation of materials making up the sample.



Figure 3.4 A photo of our SEM (Hitachi S-4800)



In most applications, data are collected over a selected area of the surface of the sample, and a 2-dimensional image is generated that displays spatial variations in these properties. Areas ranging from approximately 1 cm to 5 microns in width can be imaged in a scanning mode using conventional SEM techniques (magnification ranging from 20X to approximately 300,000X, spatial resolution of 50 to 100 nm). The SEM is also capable of performing analyses of selected point locations on the sample; this approach is especially useful in qualitatively or semi-quantitatively determining chemical compositions (using EDS) which we have been using extensively for identifying the impurities and initial analysis of our samples. The High Resolution SEM used in our group can be seen in Figure 2.4 .

Essential components of all SEMs include the following:

- Electron Source ("Gun")
- Electron Lenses
- Sample Stage
- Detectors for all signals of interest
- Display / Data output devices
- Infrastructure Requirements:
  - Power Supply
  - Vacuum System
  - Cooling system
  - Vibration-free floor
  - Room free of ambient magnetic and electric fields

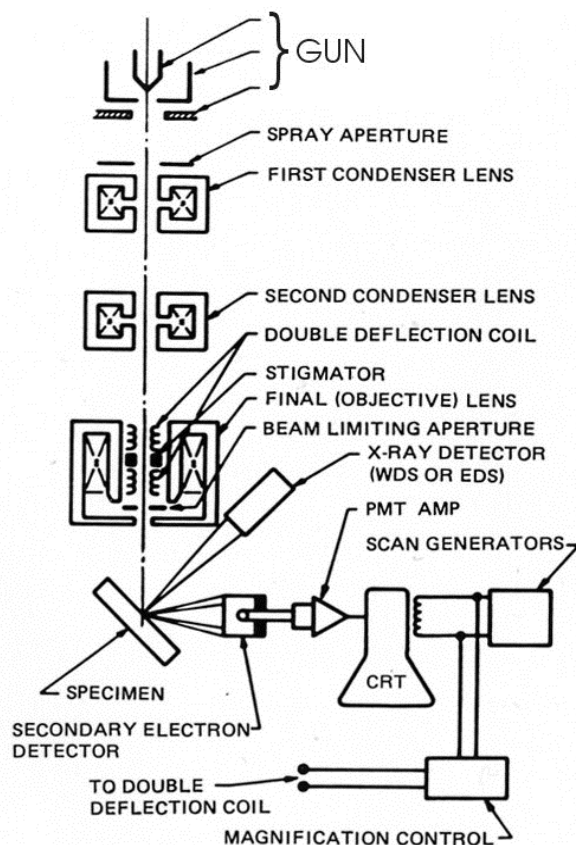


Figure 3.5 A schematic drawing of the electron and X-ray optics on a combined SEM-EPMA [1].

SEMs always have at least one detector (usually a secondary electron detector), and most have additional detectors. The specific capabilities of a particular instrument are critically dependent on which detectors it accommodates.

The morphology and composition of  $\text{NiSi}_x$  nanostructures synthesized on carbon paper, silicon wafer and Ni foam and  $\text{CoSi}_x$  nanostructures on carbon paper were characterized by Hitachi S-4500 field-emission scanning electron microscopy (SEM) operated at 5.0 kV and Energy Dispersive X-ray spectroscopy (EDX) was taken at a voltage of 20 kV.

### 2.2.2. Transmission Electron Microscope (TEM)

A TEM (transmission electron microscope) another type of electron microscope that uses a highly energetic electron beam (100 keV-1 MeV) to image and obtain structural information from thin film samples. The electron microscope consists of an electron gun, or source, and an assembly of magnetic lenses for focusing the electron beam. Apertures are used to select among imaging modes and to select features of interest for electron diffraction work.

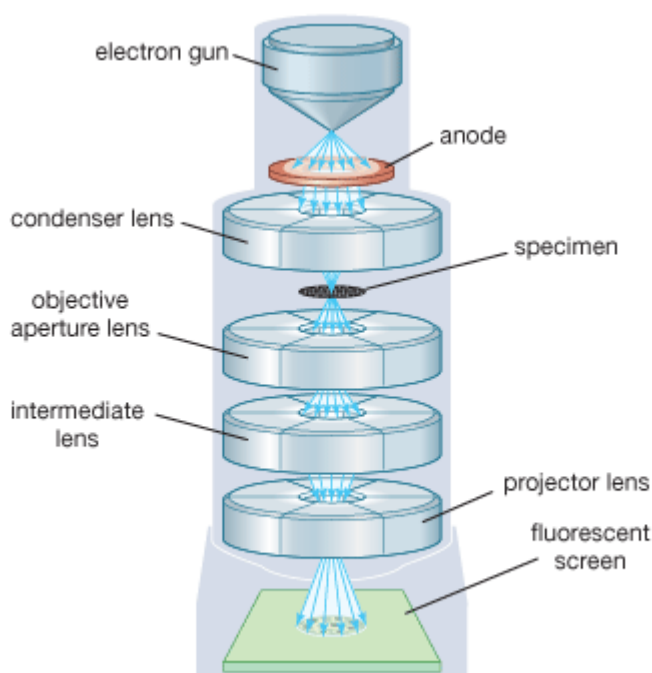


**Figure 3.6** A schematic of a TEM [2].

The sample is illuminated with an almost parallel electron beam, which is scattered by the sample. In crystalline materials, the scattering takes the form of one or more Bragg diffracted beams, which are used to form a transmission diffraction pattern. These diffraction patterns can be used to identify unknown phases in the sample. A

bright-field image of the sample can be formed by looking at the straight-through, non-diffracted beam. Features in the sample that cause scattering have darker contrast in a bright-field image than those that cause little or no scattering. An electron diffraction pattern can be generated from a particular area in a bright-field image (such as a particle or grain) by using a selected area aperture. Dark-field images are formed from a single diffracted beam and are used to identify all the areas of a particular phase having the same crystalline orientation. Magnifications from about 100x up to several hundred thousand times can be achieved in the TEM. Schematic of a typical TEM can be seen in Fig2.6 [2]. Detailed studies and analysis of single nanowires were carried out on a transmission electron microscopy (TEM, Philips CM10, 80 kV). High resolution TEM was carried out on a JEOL 2010F at voltage 200 kV to inspect the fine nanostructure. An image of the TEM used in our group can be observed in Fig2.7.



**Figure 3.7** A photo of our TEM (Philip CM10).

### 2.2.3. X-Ray Diffraction (XRD)

X-ray diffraction (XRD) is a versatile, non-destructive technique that reveals detailed information about the phase and crystallographic structure of crystalline materials. X-ray diffractometers consist of three major parts: X-ray tube, sample holder and an X-ray detector. X-rays are generated in X-ray tube by generally by heating a filament to produce electrons which are accelerated toward a target by applying a high voltage. One of the results of bombarding the target with electrons is the generation of X-ray spectra which are a characteristic of the target material. Using filters a monochromatic X-ray is isolated from the X-ray spectra and used for X-ray diffraction. Often Cu or Co  $K\alpha$  is used as the probing X-ray. The generated X-ray is focused on the sample interacting with the material. When the



Figure 3.8 A photo of Bruker D8 Advance XRD [3].

geometry of the incident X-ray impinging the sample satisfy the Bragg Equation constructive interference occurs and the X-ray detector records the diffracted X-ray signals and converts them to counts.

The structure and phase of the  $\text{NiSi}_x$  and  $\text{CoSi}_x$  were investigated and determined by analysing the XRD pattern which were recorded on a Bruker D8 Advance diffractometer (Fig2. 7) equipped with a Co  $K\alpha$  radiation source.

## References

1. **Goldstein, J.** (2003). Scanning electron microscopy and x-ray microanalysis. kluwer Academic/plenum publishers .
2. *Encyclopedia Britannica.* (n.d.). Retrieved from <http://www.britannica.com/EBchecked/media/110686/Transmission-electron-microscope>
3. *Bruker-axes.* (n.d.). Retrieved from [http://www.bruker-axes.com/d8\\_advance.html](http://www.bruker-axes.com/d8_advance.html).

## **Chapter 4 Controlled synthesis and growth mechanism of NiSi<sub>x</sub> nanowires by chemical vapor deposition**

### **Abstract**

Free standing, crystalline NiSi<sub>x</sub> nanostructures were fabricated using chemical vapor deposition method. Silicon powder and different nickel based powders were used as source material. The nanostructures were characterized SEM, TEM, and XRD techniques. A systematic study on the growth of Ni<sub>2</sub>Si nanostructures indicates that the morphology and composition of the synthesized nanostructures are sensitive to growth factors such as substrate morphology and source material. SEM and TEM observations demonstrated the morphology of core shell nanowires with diameters between 50 to 300 nm on these substrates. Vapor-solid mechanism and vapor-liquid-solid mechanism were proposed for the growth of NiSi<sub>x</sub> nanostructures and SiO<sub>x</sub> branched nanostructures respectively. These nanostructures are expected to be potential candidates in energy related applications such as lithium ion batteries and silicon based nanodevices.

### **3.1. Introduction**

Transition metal silicides have been extensively investigated due to their applications in conventional integration technologies in the past decades. With the increasing demand for

---

Note: This will be revised and submitted for publication

Hamid Norouzi Banis<sup>1</sup>, Yong Zhang<sup>1</sup>, Mohammad Norouzi Banis<sup>1</sup>, Ruying Li<sup>1</sup>, Mei Cai<sup>2</sup> and Xueliang Sun<sup>1</sup>,  
1. Department of Mechanical and Materials Engineering, The University of Western Ontario, London,  
Ontario N6A 5B9 (Canada)  
2. General Motors R&D Center, Warren, MI 48090-9055 (USA)

highly integrated devices, development of nanostructured metal silicides bestows a promising way to achieve ideal building blocks with higher device densities than the conventional semiconductor technology cannot provide. The bottom-up approach for synthesizing nanostructures provides an effective way to grow 1D systems such as nanowires (NWs) and nanorods, and transition metallic silicide nanowires obtained in this way have been proved as promising candidates for various future applications [1-5] due to their diverse properties such as low resistivity, good ohmic contacts with p- and n-type semiconductors, high-thermal stability, low cost, and compatibility with the processing of Si devices. Most noted of these applications are interconnect, gate materials for CMOS microelectronic transistors [6], fuel cell and lithium ion batteries[7-11].

Among various metal silicides, nickel silicide is currently one of the most promising silicide materials because of its superior electrical properties and appropriate work function. Some Ni-rich silicides, such as  $\text{Ni}_2\text{Si}$  and  $\text{Ni}_{31}\text{Si}_{12}$  have gained much attention for use in *P* type MOS devices because of their higher work functions (4.8 eV)[12-13]. Because of these potential applications several methods have been adopted to synthesize metal silicide nanostructures on different substrates such as silicidation of Ni-coated Si NWs [14], metal-induced growth [15-16], point contact reaction between Si and Ni NWs [17] and chemical vapor deposition [18-20]. Although many of the strategies used for synthesizing NiSi have had low rate of production or synthesized in a free standing form for silicon based devices and few have been employed for energy applications. In energy applications such as fuel cells and lithium ion batteries there is a need for a highly dense production of nanostructures on specific substrates that can be



used in an industrial scale. CVD method has been proposed to obtain this goal in previous works [20-22].

Many of these reports given for the synthesis of  $\text{NiSi}_x$  nanostructures have been carried out by delivering silicon in vapour form to the Ni substrate. The chemical compounds used for silicon are highly corrosive and dangerous to work with. In this study we have successfully synthesized  $\text{NiSi}_x$  using CVD method using solid based precursors. The growth of these nanostructures and parameters affecting their morphology has been systematically studied. A growth mechanism is proposed based on the experimental results.

### **3.2. Experimental details**

$\text{NiSi}_x$  nanowires were synthesized on different substrates using a CVD method. Schematic diagram of the synthesis set up is shown in Fig 3.1. As seen the  $\text{NiCl}_2$  was placed near the entrance at a temperature zone of  $500\text{ }^\circ\text{C}$ . Silicon powder (99.9%) was put in the alumina boat as the silicon source as opposed to other reports which use a constant flow of silane or  $\text{SiH}_4$  gas [22-24]. The silicon powder was positioned in the center section. Ni foam, silicon wafer and carbon paper have been studied as the substrates. Silicon wafer and Ni foam were sonicated in HCl acid and acetone for 10min, respectively. A  $5\text{mm} \times 10\text{mm}$  substrate was kept at a distance of 2mm over the silicon powder. The synthesis was carried out under 200 sccm of Ar. The temperature of the furnace was raised to around  $900\text{ }^\circ\text{C}$  and kept at this temperature for 1hr. At the end of synthesis process, a dark layer is deposited on the substrate.

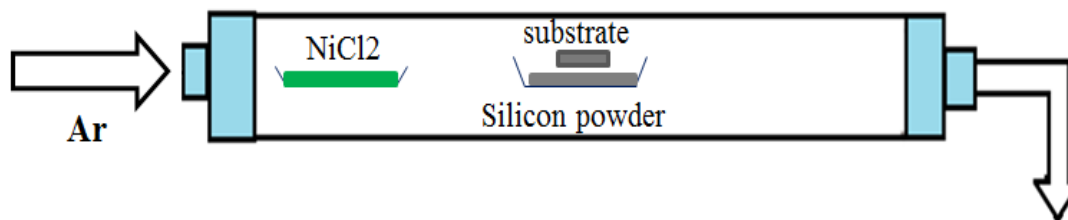


**Figure 4.1 Schematic diagram of the nickel silicide synthesis process**

The morphology, structure and composition of the resultant products were characterized by Hitachi S-4500 field-emission SEM operated at 5.0 kV and energy dispersive X-ray spectrometer (EDX), Rigaku–Miniflex X, using CuK $\alpha$  ( $k = 0.154$  nm) radiation operated a 30 kV and 15 mA, Philips CM10 transmission electron microscope (TEM) and selected area electron diffraction (SAED) operated at 80 kV, a Jeol 2010 field emission gun high resolution electron microscope (HRTEM) operated at 200 kV and Kratos Axis Ultra Al (alpha).

### **3.3. Results and discussion**

NiSi nanowires were synthesized using a single zone CVD method. The morphology of nanostructures after optimization of the growth parameters are shown in the SEM images of Fig3.2(a-b). The length and density of the grown nanowires are quite unique compared to previous reports [24-26]. As shown in Fig3.2(a) high density coverage of nanowires is deposited on the substrate. These nanowires have lengths up to 300  $\mu\text{m}$  and an average diameter of 250 nm Fig3.2(b). SEM observations of the cross section view of the products grown on the silicon substrate reveal that the nanowires growth is after the formation of bundles on the substrates.

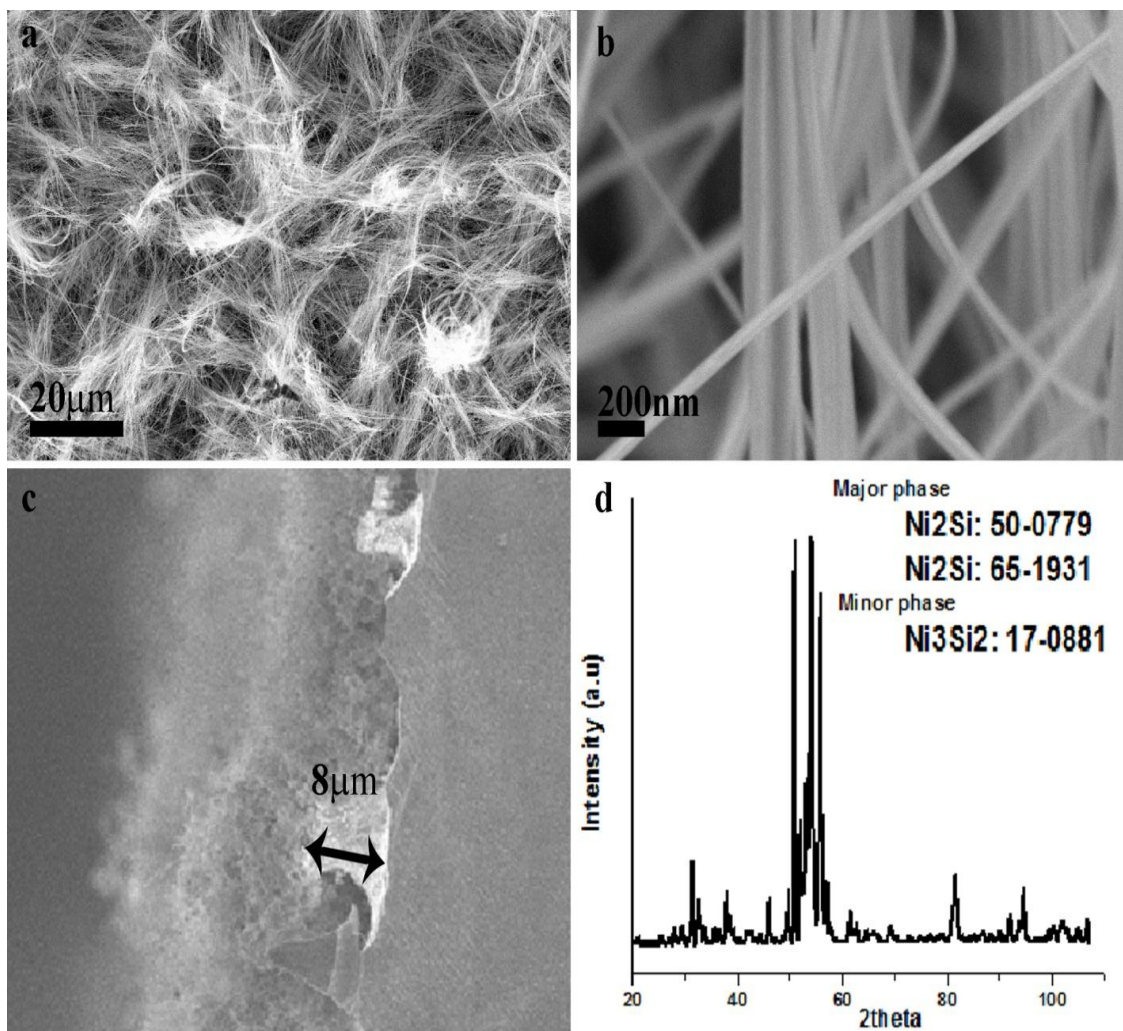


**Figure 4.2** HRSEM image of  $\text{Ni}_2\text{Si}$  nanowires. (a) low magnification (a) High magnification (b) cross section view. the thickness of the bundles are around 5-10  $\mu\text{m}$  (c) XRD pattern of these nanowires on a silicon substrate.

EDX indicates these bundles are composed of silicon, nickel and oxygen. The thickness of these islands is around 5 to 10  $\mu\text{m}$ . The main diffraction peaks in the XRD pattern of these nanowires shown in Fig3.2(d) can be assigned to the  $\text{Ni}_2\text{Si}$  indicating that the nanowires have well-crystallized  $\text{Ni}_2\text{Si}$  structure. In addition to  $\text{Ni}_2\text{Si}$ , weaker peaks can be attributed to  $\text{Ni}_3\text{Si}_2$ .

TEM image of a single Ni<sub>2</sub>Si nanowire is shown in Fig. 3(a). TEM observations indicate that these nanowires have a core-shell structure with a crystalline core covered by an amorphous layer. Detailed measurements on TEM images reveal that the nanowires have a core diameter of around 190 nm and the shell thickness of 60 nm. EDX analysis, (inset in Fig.3.3(c)) reveals that the nanowires are composed of nickel, silicon and oxygen. It was found that lower working pressure has a noticeable effect on the reduction of the oxide shell [27]. The SAED pattern recorded from the core shown in Fig3.3(b), reveals a well ordered spot diffraction revealing the single crystalline nature of the core of these nanostructures. The SAED pattern of the core can be fully indexed to Ni<sub>2</sub>Si orthorhombic crystal structure confirming the results obtained from XRD pattern. Based on the SAED pattern and the EDX analysis of the nanowires, the amorphous layer is determined to be composed of silicon oxide (SiO<sub>x</sub>).

During our experimental process we have found that the morphology and crystal structure of the nanowires is very sensitive to the growth parameters such as temperature, substrate, time and composition of the carrier gas. In order to control the morphology of the Ni<sub>2</sub>Si nanostructures and understand their growth mechanism, the effect of these growth parameters were systematically studied.

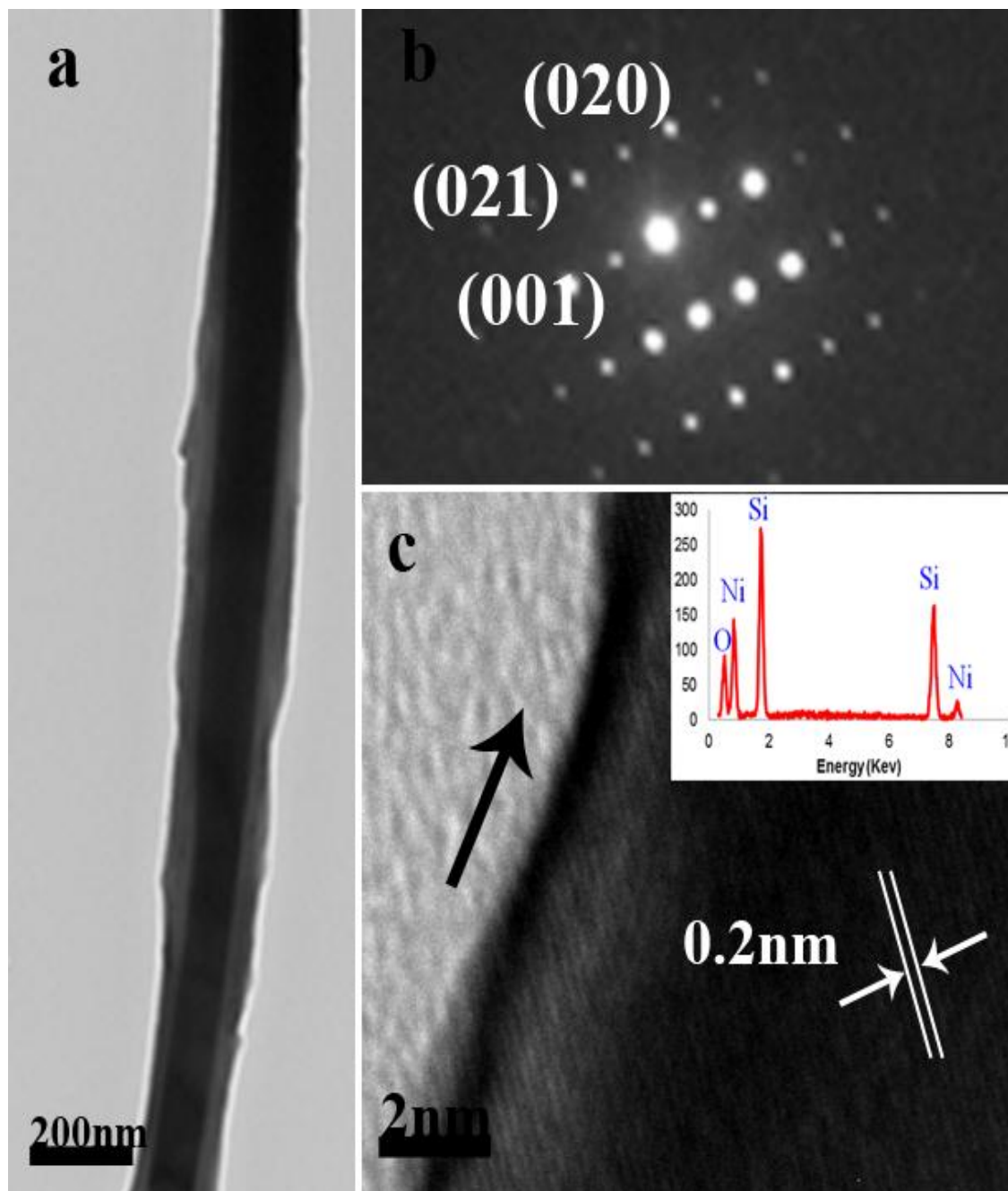
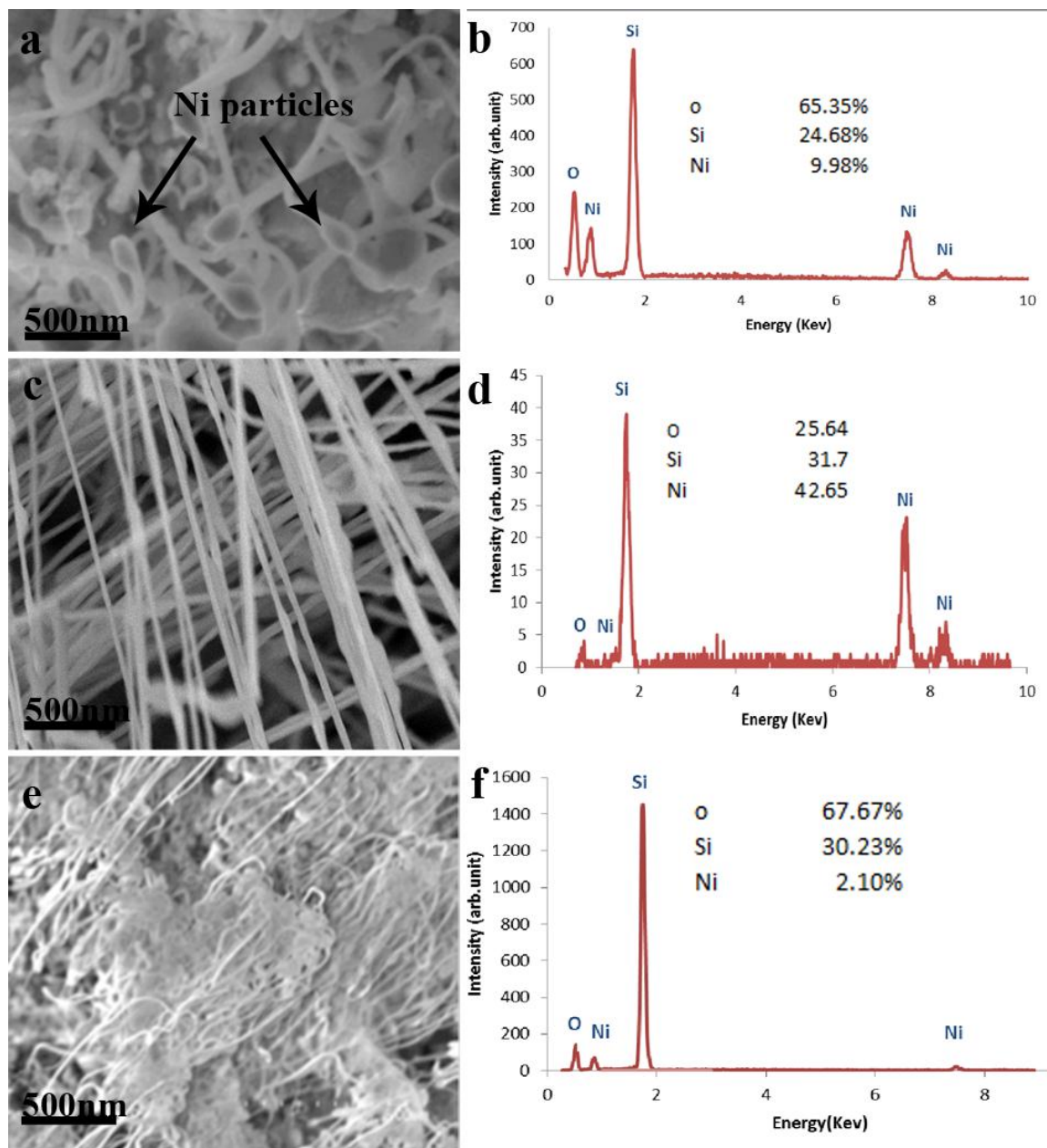


Figure 4.3 (a) TEM image of a single Ni<sub>2</sub>Si nanowire with a diameter of about 250 nm. (b) Corresponding SAED pattern (c) HRTEM of the NW and EDX analysis of these nanowires (inset).

### 3.3.1. Temperature effect

Temperature was found to have a significant impact on the morphology and composition of the nanostructures. The effect of temperature on the growth was investigated from 850 °C to 950 °C. As shown in Fig. 4(a), at low temperatures, amorphous nanowires were formed on the substrate. Small nanoparticles can be seen on top of these nanowires which indicate the catalyst effect of these nanoparticles. EDX analysis (Fig. 4(b)) reveal that there is a high amount of silicon and oxygen concentration compared to nickel. Increasing the temperature to 900 °C resulted in the formation of highly dense product of Ni<sub>2</sub>Si nanowires with lower oxygen content as shown in Figure 4(c-d). However the experimental results reveal that further increase of temperature is unfavorable for the formation of nickel silicide nanostructures. Figure 4(e) shows the SEM images of nanostructures synthesized at 950 °C. EDX analysis shows a high level of oxidation with very low percentage of Ni as opposed to previous conditions. The charging effect seen in SEM image shown in Fig. 4e indicates the low conductivity of the products due to abundant SiO<sub>x</sub> and lack of conductive Ni. At a lower temperature of 850 °C, partial pressure of nickel reactive species is not high enough to trigger the nucleation of nickel silicide, hence, the generated nickel clusters act as catalysts for the growth of silicon and silicon oxide nanowires via a vapor-liquid-solid mechanism as reported previously [28]. This mechanism often has a characteristic catalyst nanoparticle at the tip of the grown nanowires as seen in Fig3.4a unlike nanostructures synthesized at higher



**Figure 4.4** SEM and EDX spectrum of nanostructures synthesized on silicon wafer at (a, b) 850 °C (c, d) 900 °C (e, f) 950 °C.

temperatures. At a higher temperature of 900 °C, partial pressure of nickel species reaches the level for nucleation and growth of nickel silicide thereby leads to the growth of nickel silicide nanowires. With further increase of the temperature to 950 °C, elevated partial pressure of oxygen inside the chamber system enhances the growth of silicon oxide which

inhibits the growth of nickel silicide. Therefore, the synthesis temperature has to be carefully controlled in a narrow range to guarantee the smooth growth of nickel silicide nanowires.

### 3.3.2. Substrate effect

In terms of practical applications, role of substrates has to be dealt with for nanowire growth. In our work, it was found that the morphology of  $\text{Ni}_2\text{Si}$  nanowires synthesized via CVD method varies depending on the morphology and composition of substrates. In this study the effect of some substrates such as silicon wafer, carbon paper and Ni foam were studied. Fig 3.5 shows the products obtained on carbon paper and nickel foam (please double check the caption of Fig3.5). As seen in Fig3.5(a) the nanowires grown on carbon paper have a similar morphology to nanostructures synthesized on silicon substrate (Fig3.1(a)). However these nanowires have an average diameter of 380 nm and length up to 100  $\mu\text{m}$ , which is larger and shorter than nanowire synthesized on silicon wafer. Furthermore, the nanostructures synthesized on carbon paper had a higher density and uniform diameters. In addition, these nanowires exhibited stronger binding to the substrate compared to the nanowires on silicon wafer which could be detached easily. As shown in Fig3.5(b), XRD pattern of nanostructures synthesized on carbon paper, indicates that nanowires produced on both carbon and silicon substrates have similar crystal structure. This indicated that the silicon wafer substrate didn't have evident influence on the reaction for nanowire growth. But for the Ni foam substrate, the experimental results were rather completely different in not only the morphology but also the crystal structure of the nanowires, as shown in Fig3.5(c). XRD result in Fig3.5(d) indicates the presence of  $\text{Ni}_{31}\text{Si}_{12}$  in the products grown on the Ni foam substrate. The growth of nickel-rich nickel



silicide indicates the possible contribution of Ni foam to the synthesis of nickel silicide crystal structures. The nanostructures synthesized on Ni foam as seen in Fig. 5(c), although the majority of the nanowires grown on the Ni foam are silicon oxide as a result of the oxide layer present on the Ni foam. Compared to the nanowire on silicon and carbon paper substrates, these nanowires have smaller diameters of around 80 nm and lengths of more than 20  $\mu\text{m}$ ,

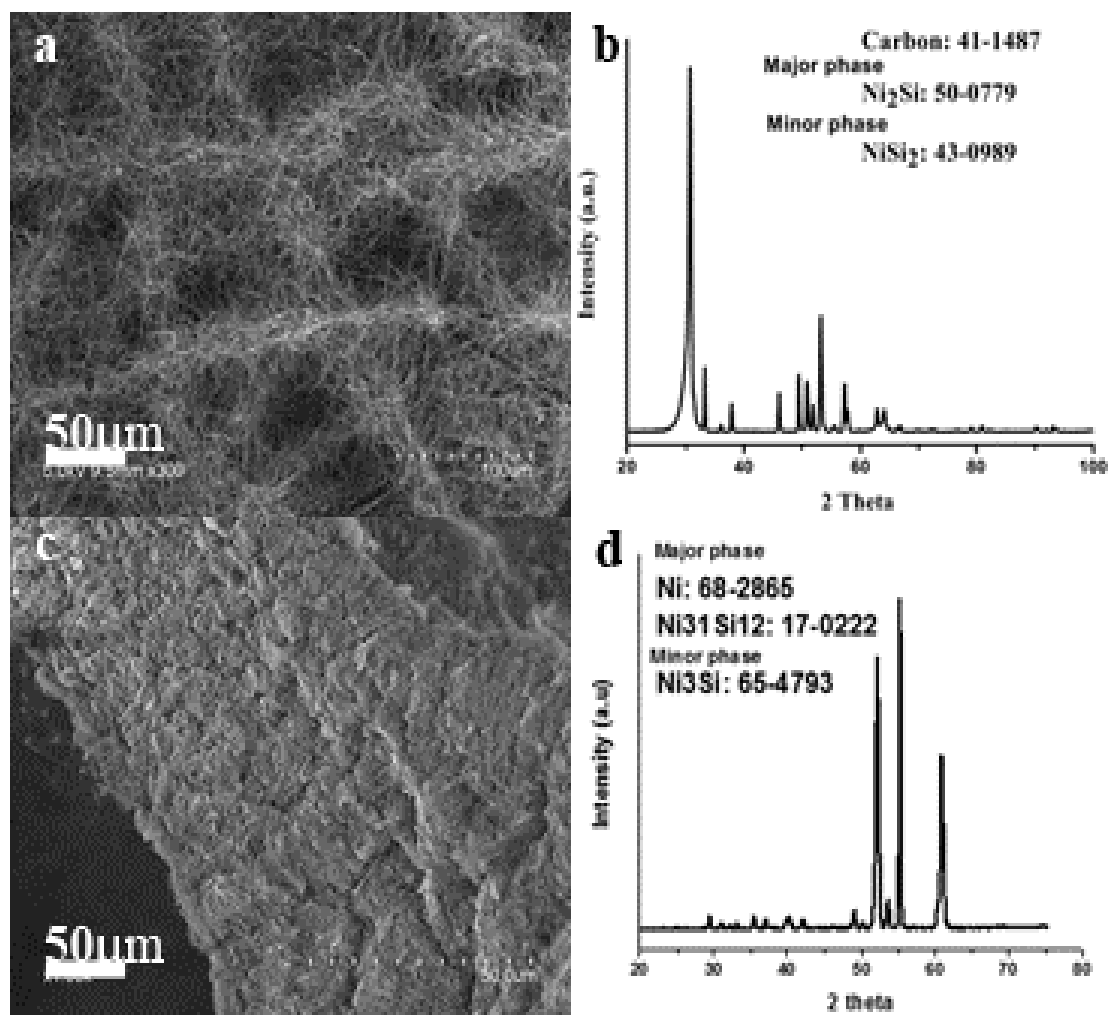


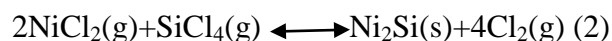
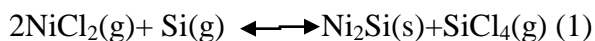
Figure 4.5 SEM and XRD pattern of NiSix NWs growth on (a, b) carbon paper (c,d) Ni foam.

### 3.3.3. Growth mechanism

Based on the investigation on the morphology evolution of the products, growth mechanism of the nickel silicide nanowires is proposed and can be divided into four stages as schematically shown in Fig. 6(a), and corresponding SEM morphology images are shown in Fig3.6(b-e). In the initial stage, as seen in Fig3.6(b), nucleation occurs in the form of conical shaped nano particles possibly due to fast diffusion of Ni into silicon and generation of initial nickel silicide nuclei. The composition of these clusters is not clear. However the XRD pattern shown in Fig3.1(b) reveal the presence of small amount of  $\text{Ni}_3\text{Si}_2$  having higher silicon to nickel ratio may provide nucleation sites for  $\text{Ni}_2\text{Si}$  nanowire growth on the silicon substrate. At the second step as observed in Fig3.6(c), rate of Ni deposition is comparable to rate of silicon diffusion into the clusters, creating an elongated structure which ultimately resulted in the appearance of nanowires on the conical nanoparticles. In the next stage, nanowires propagate during the growth (Fig3.6(d)). As the time is extended, the annealing causes the nanowires to have a finer structure. By comparing the two last stages, it is apparent that in some areas Ni-Si nanoparticles are formed due to non-uniform accumulations of the reactive species.

The formation of nickel silicides was found to depend on the ratio of Ni and Si species in the CVD chamber. Ni atoms are known to be the dominant diffusing species in the Ni-Si reactions. It has been reported that the probability of  $\text{Ni}_2\text{Si}$  phase nucleation in Ni-Si reactions is higher compared to other phases because it is the most thermodynamically stable phase [27]. In this study,  $\text{NiCl}_2$  powder was introduced in front of the substrate. This leads to reaction of Si vapour from the source zone with the  $\text{NiCl}_2$

vapour to form single-crystal  $\text{Ni}_2\text{Si}$  NWs at the middle zone in the furnace. The probable reaction pathways are the following [27]:



It is worthwhile to mention that the  $\text{NiCl}_2$  vapour plays two roles. Primarily, the vapour of  $\text{NiCl}_2$  can react with the Si vapour to produce  $\text{NiSi}_x$  nanostructures. Second, excessive  $\text{NiCl}_2$  can also react with the Si vapour to form  $\text{SiCl}_4$  which is a highly reactive compound and can promote the  $\text{NiSi}_x$  deposition.

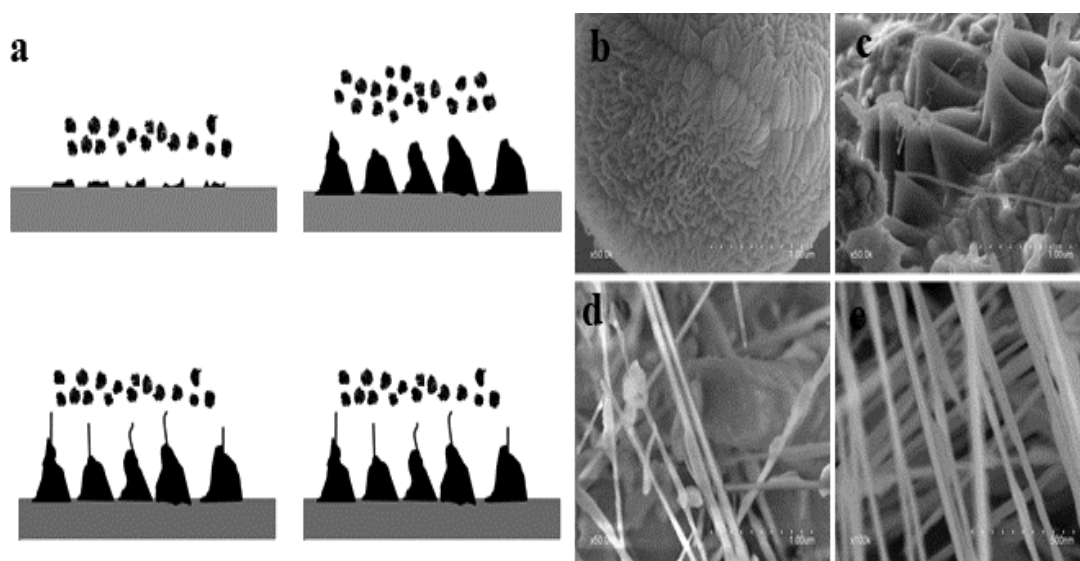


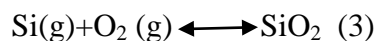
**Figure 4.6** (a) Schematic diagram of the NW heterostructures growth. HRSEM image of time dependent growth of nanostructures: (b) 30min; (c) 1hr; (d) 1:15hr; (e) 1:45hr.

Due to high melting point of silicon which is  $1414\text{ }^\circ\text{C}$ , the nickel-rich and silicon-poor atmosphere tends to be created in the reaction chamber, which may explain the reason why nickel-rich  $\text{Ni}_2\text{Si}$  nanowires were obtained. Effect of nickel precursor amount

on the growth was also investigated by placing different amounts of  $\text{NiCl}_2$  powders (200-800 mg) on the upstream of the substrates. Results show that higher amount of  $\text{NiCl}_2$  (>300 mg) leads to predominant etching of the substrate (excess chlorine) which inhibits the nanowire growth on the substrate [27]. On the other hand, at lower quantities of  $\text{NiCl}_2$  powders (<200 mg), no nanostructures were observed on the substrates. The optimal weight range was found to be between 200 and 400 mg.

As discussed above, temperature plays a crucial role in dominating phase structure and composition of the products. At lower temperatures around 800 °C, Ni indeed acts as a catalyst to form  $\text{SiO}_x$  nanowires via a vapour liquid solid mechanism based on previous reports on the catalytic effect of Ni for the growth of  $\text{SiO}_2$  nanostructures [28,29]. In this case, partial pressure of nickel reactive species is relative low and the formation of silicon oxide nanostructures is the consequence of a lack of appropriate activation energy for triggering the nucleation and growth of nickel silicide. At a higher temperature of 900 °C, partial pressure of nickel species reaches the level for nucleation and growth of nickel silicide thereby leads to the growth of nickel silicide nanowires. With the increase of the temperature over 950 °C, high amount of silicon oxide was grown on the substrate. (This can be the outcome of two factors. Firstly it can be explained by the fact that at these high temperatures the amount of nickel vapour deposition on the substrate is low. This can be confirmed by the EDX results in Fig3.4(f). Secondly With increasing temperature, partial pressure of oxygen was elevated, which inhibited the growth of nickel silicide while enhanced the growth of silicon oxide. In our experiments, it seems all three of these reactions (1), (2) and (3) are taking place since we have both  $\text{Ni}_2\text{Si}$  component as the core

in the nanowires and silicon dioxide formation as the shell, while silicon vapour is consumed in a faster reaction which is [30]:



In all the three substrate that have been investigated the synthesis mechanism has been a nucleation growth and vapor solid (VS) mechanism. In silicon wafer the nucleation shows itself as agglomeration of Ni and silicon into a large bundle as shown in Fig3.1(c). In other substrates, these agglomerations are much smaller presumably due to the fiber structure of Ni foam and carbon paper.

#### 4. Conclusion

In summary, high quality nickel silicide nanowires were synthesized using a CVD process on different substrates such as silicon, Ni foam and carbon paper with high density and lengths of up to 100µm. XRD pattern indicated the nanostructures synthesized on silicon wafer and carbon paper have a Ni<sub>2</sub>Si crystal structures and nanostructures deposited on Ni foam have a Ni<sub>2</sub>Si<sub>3</sub> crystal structure. TEM analysis revealed the core-shell morphology of these nanowires with average diameters of around 300 nm. EDX analysis confirmed the presence of silicon oxide shell on the nickel silicide nanowires. The effects of various growth parameters on the morphology of nanostructures deposited were systematically studied. Based on these experimental results VS method was proposed as the dominant growth mechanism for Ni<sub>2</sub>Si nanostructures. This study clarifies the important parameters for the growth of crystalline NiSi<sub>x</sub> which may have great potential in various nanostructured system such as interconnects in nanodevices, as catalyst support in fuel cells and anode material in lithium Ion batteries

## References

1. **Chen, L. J.** 2007, JOM, pp. 57(9), 24-30.
2. **V Chakrapani, F Rusli, M A. Filler, P A. Kohl.** 2005, J power sources , pp. 205,433-438.
3. **J H Cho, X Li, S. T Picraux.** 2012, J power sources, pp. 205 ,467-473.
4. **K. Kang, K. Song, H. Heo, S. Yoo, G. Kim, G. Lee, Y. Kang, M. Jo.** 2011, Chem Sci, p. 1090.
5. **S. L. Zhang, M. Ostling.** 2003, crit. Rev. solid Matter, pp. 28,1-129.
6. **Y. J. Hu, J. Xiang , G. C. Liang ,H. Yan,C. M. Lieber.** 2008, Nano lett., pp. 8,925-930.
7. **Maszara, W. P.** 2005, J Electrochem. Soc., pp. 152,G550-G555.
8. **K. Kang, K. Song, H. Heo, S. Yoo, G. Kim, G. Lee, Y. Kang, M. Jo.** 2011, Chem Sci. , pp. 2,1090.
9. **H. Zang, F. Li, C. Liu , H. Cheng.** 2008, Nanotechnology, pp. 19,165606.
10. **Chan C K, Peng H, Liu G, Mcilwrath K, Zhang X F, Huggins R A and Cui Y.** 2007, Nat. Nanotechnology , p. doi:10.1038/nnano.2007.411.
11. **Wang G X, Sun L, Bradhurst D H, Zhong S, Dou S X and Liu H K.** 2000, J. Alloy Compounds, pp. 306,249-252.
12. **Wang Z, Tian W H, Liu X H, Li Y and Li X G.** 2006, Mater. Chem. Physics, pp. 100, 92-7.
13. **Maszara, W. P.** 2005, J. Electrochem. Soc., pp. 152,G550.
14. **Kittl J. A., Lauwers A., Veloso, A., Hoffmann T., Kubicek S., Niwa M. van Dal, M. J. H., Pawlak M. A. Brus S., Demeurisse C., Vrancken C., Absil P., Biesemans S.** 2006, IEEE Electron Device Lett., pp. 27,966-968.
15. **C. Lee, M. Lu, K. Liao, W. Lee, C. Huang, S. Chen, and L. Chen.** 2006, J phys. Chem. C, pp. 113,2286-2289.
16. **Wu Y, Xiang J, Yang C, Lu W and Lieber C M.** 2004, Nature, pp. 430 ,61-5.
17. **Kim C J, Kang K, Woo Y S, Ryu K G, Moon H, Kim J M, Zang D S and Jo M H.** 2007, Adv. Mater., pp. 19 3637-42.
18. **Kim J D, Anderson W A, Song Y J and Kim G B.** 2005, Appl. Phys. Lett., p. 86 253101.

19. **Lu K C, Tu K N, Wu W W and Chen L J.** 2007, App. Phys. Lett, pp. 90, 253111.
20. **Kim J, Lee E S, Han C S, Kang Y, Kim D and Anderson W A.** 2008, Microelectron Eng., pp. 85, 1709-12.
21. **G, Iriarte F.** 2011, Appl. Phys., pp. 11 82-6.
22. **G, Iriarte F.** 2010, J Non-Cryst Solid, pp. 356 1135-1144.
23. **C.-J. Kim, K. Kang, Y. S. Woo, K.-G. Ryu, H. Moon, J.-M. Kim, D.-S. Zang and M.-H. Jo.** 2007, Adv. Mater, pp. 19,3637.
24. **x.q. yan, h.j. yuan ,j.x.wang ,d.f. liu ,z.p. zhou ,y. gao ,l. song ,l.f. liu ,w.y. zhou ,g.wang ,s.s. xie.** 2003, Appl. Phys., pp. 79,1853-1856.
25. **Song Y, Schmitt AL, Jin S.** 2007, Nano Lett. , pp. 7(4) 965-9.
26. **Z. Zhang, J. Lu, P.-E. Hellström, M. Östling, and S.-L. Zhang.** 2006, Appl. Phys., pp. 88,213103.
27. **C. Lee, M. Lu, K. Liao, Wei-Fan Lee, C. Huang, S.Chen, and L. Chen.** 2009, J. Phys. Chem. C., pp. 113,2286-2289.
28. **J. Zheng, X Song, X. Li, and Y. Pu.** 2008, J phys. Chem., pp. 112, 27-34.
29. **X. M. Cai, a\_ A. B. Djurišić, and M. H. Xie.** 2005, J. App. Phys. , pp. 98,074313.
30. **P. Sharma, J. V. Anguita, V. Stolojan, S. J. Henley and S. R. P. Silva.**

## **Chapter 5 Synthesis of CoSi nanowires using chemical vapor deposition method at different ambient pressure levels**

### **Abstract**

With the need for higher performance and stability in energy applications there have been extensive studies on the use of nanomaterials in this field. We report the synthesis of high density CoSi nanowires using single zone CVD method on carbon paper. The use of separate solid precursors enabled the synthesis of NWs at different pressure levels in the synthesis chamber and temperatures. Optimization of the products at low pressure and atmospheric pressure resulted in the growth of two types of crystalline and core-shell nanowires. The length and diameter of the NWs synthesized at atmospheric pressure were relatively larger than NWs at low pressure. XRD and EDX confirm the deposition of CoSi nanostructures at both pressures.

### **4.1. Introduction**

In recent years, one-dimensional nanocable heterostructures have drawn much attention due to their unique properties which has led to extensive research on their synthesis, formation mechanisms, properties and applications [1-11]. Among these nanostructures silicide materials have attracted a great deal attention for their low resistivity which is

---

Note: This will be revised and submitted for publication

Hamid Norouzi Banis<sup>1</sup>, Yong Zhang<sup>1</sup>, Mohammad Norouzi Banis<sup>1</sup>, Ruying Li<sup>1</sup>, Mei Cai<sup>2</sup> and Xueliang Sun<sup>1</sup>,  
1. Department of Mechanical and Materials Engineering, The University of Western Ontario, London,  
Ontario N6A 5B9 (Canada)

2. General Motors R&D Center, Warren, MI 48090-9055 (USA)



highly desirable for silicon based devices and physical properties which make them compatible and suitable for energy application and future electronic devices [12-18]. In the current advancements in the study of silicide based applications, cobalt silicides have served essential role as ohmic contacts and interconnect materials and gates in VLSI and ULSI CMOS processes because of their compatibility[19,20]. Researchers have shown that the resistivity of the CoSi thin film on a Si(001) substrate and the bulk single-crystal CoSi is 350 and 180  $\mu\Omega\cdot\text{cm}$ , respectively [21,22]. On the other hand, CoSi NWs were found to possess a resistivity ranging from 126.5 to 510  $\mu\Omega\cdot\text{cm}$  [56]. Furthermore Silicide nanostructures have also been studied as catalyst and anode materials fuel cell and lithium ion batteries respectively [24-27]. CoSi nanostructures can also be potential candidates for these energy based applications.

Synthesis of CoSi nanowires have been reported using chemical vapour deposition (CVD) [57] and chemical vapour transport (CVT). In these methods a silicon substrate or a Co coated substrate chemically reacts with the metal or the silicon source [11, 28-31] . There have been many numbers of reports of synthesis of metal silicide using this method [32-36]. Lion et al. used this approach to synthesize FeSi nanowires using  $\text{FeCl}_3$  as precursor [58]. These methods have the disadvantage of inflexibility where the choice of the substrate is limited and there is less control on the ratio of the elements in the product nanowires.

The use of single source precursors (SSP) have been proposed [38,39] where both the metal and silicon have been mixed and used as a single source large molecule. Although in these reports they have managed to produce desired  $\text{CoSi}_x$  nanostructures, this method adds an additional step to the synthesis process. To achieve good chemical

control in the nanophase formation of CoSi, we have strived to deliver both the metal and silicon elements via the vapour phase separately using CVD. This method has proven to be very simple and inexpensive and yet allows much more control on the deposition and reaction of the two elements of the silicide material.

Here we report the successful growth of CoSi nanowires in ambient and low pressure by optimizing the conditions of the system.

#### 4.2. Experimental procedure

CoSi nanowires were synthesized in a single zone furnace through a CVD process.  $\text{CoCl}_2$  was used as the precursor for Co source and silicon powder (325 mesh-99%) was used for silicon source. Carbon paper with different thicknesses were used as the substrates.

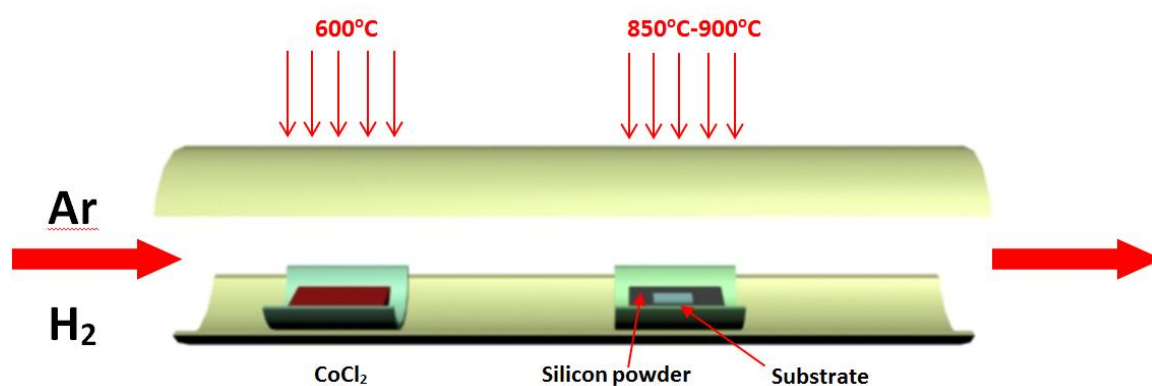


**Figure 5.1** Schematic diagram showing the setup of substrate and the sources in Quartz tube of CVD process for the synthesis of CoSi nanowires.

As shown in Fig4.1 the substrate was positioned at the center of the heating section with a 2 mm distance from the silicon powder.  $\text{CoCl}_2$  was situated at temperature zone around 450-550°C at upstream of the furnace according to the center heating

temperature and pressure of the experiments in order to achieve gradual evaporation of the precursor at the set condition. Initially Ar (99.99%) was introduced into the CVD chamber for 30 min to remove the residual oxygen in the system. To study the effect of CVD chamber pressure on the growth of cobalt silicide nanostructures the pressure of the synthesis chamber was reduced using a mechanical pump and the chamber pressure was adjusted by continuous flow of Ar gas which also acted as the carrier gas. The temperature was increased to the set temperature and held at this temperature for 2 hours. At the end of the experiment a dark layer was deposited on the substrates.

The samples were characterized by Hitachi S-4500 field-emission scanning electron microscope (SEM) operated at 5.0 kV and energy dispersive X-ray spectrometer (EDX), Bruker D8 X-ray diffractometer using Co Ka( $\lambda = 0.154$  nm) radiation operated at 45 kV and 30 mA, Philips CM10 transmission electron microscope (TEM) and selected area electron diffraction(SAED) operated at 80 kV, a Jeol 2010 field emission gun high resolution electron microscope (HRTEM) operated at 200 kV and Kratos Axis Ultra Al(alpha).

### **4.3 Results and discussion**

Cos<sub>2</sub> nanowires were synthesized using chemical vapour deposition. To have a better understanding of their growth mechanism, the effect of various growth parameters such as CVD chamber pressure and temperature on the morphology of the nanostructures deposited on the substrate were investigated.

## CVD Chamber Pressure

In atmospheric pressure the optimized temperature of the center furnace was found to be 850 °C with  $\text{CoCl}_2$  placed at a temperature zone of around 550 °C. The growth time was adjusted to 2 hours which led to the formation of nanowires covering the entire fibers of a  $1 \times 0.5 \text{ cm} \times \text{cm}$  carbon paper substrate as shown in Fig4.2. The low magnification SEM image (Fig4.2a) indicate that the nanowires have a rather high density.

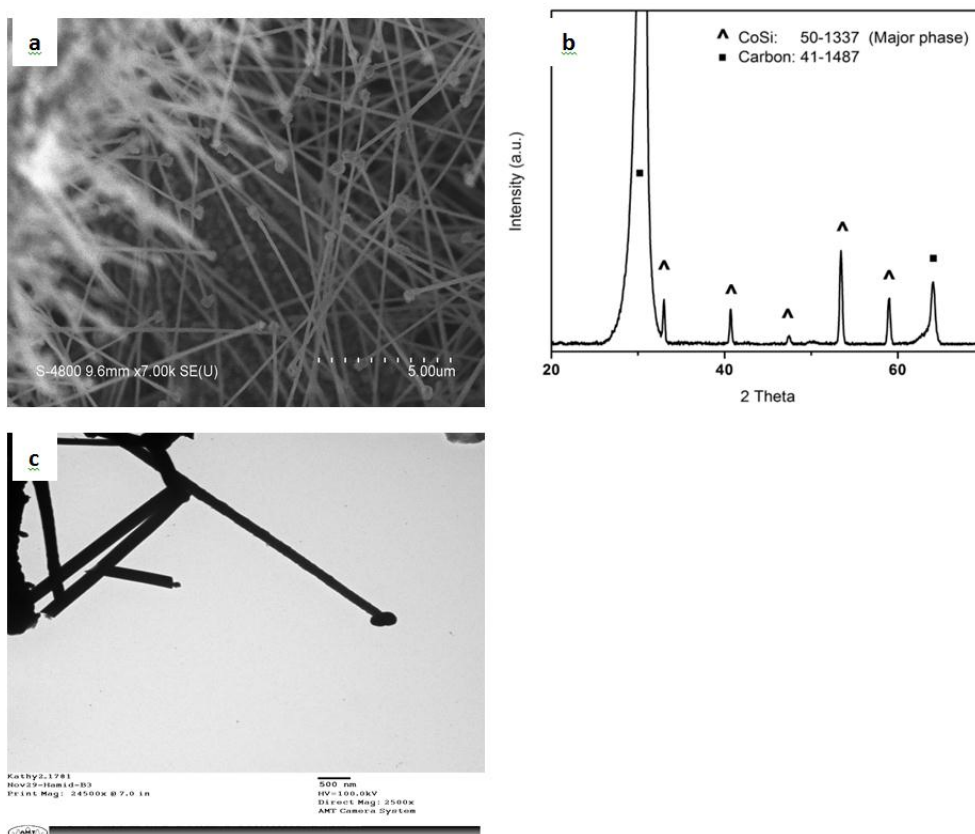


Figure 5.2 (a) HRSEM at 850 °C in atmospheric condition; (b) XRD pattern; (c) TEM image of single nanowire; (d) HRTEM of CoSi nanowire (inset is SAED pattern).

It is also observed that the nanowires have particles on the top which suggests that the CoSi nanowires were grown via vapour-liquid-solid (VLS) mechanism and since no

additional material was used for catalyst it is apparent that it has to be a self-catalysis process (Fig4.2a,c). Fig4.2(b) displays the XRD pattern of the products on the carbon paper substrate. The main diffraction peaks are assigned to the cubic CoSi structure.

TEM observations of a CoSi nanowire can be seen in Fig4.2c. Analysis of these nanowires under TEM showed that the nanowires have diameters around 150-100 nm with lengths up to tens of micrometers. Furthermore, the TEM images indicate that these nanostructures have a core shell morphology. Detailed analysis of these nanostructures reveal the core section to be crystalline covered by an amorphous layer with comparable thickness. EDX analysis on the nanostructures show the presence of oxygen in the nanostructures which can be the results of amorphous SiO<sub>2</sub> formation around the CoSi nanowires.

There have been a number of reports on the synthesis of CoSi nanowires using CVD process at pressures as low as  $1 \times 10^{-3}$  Torr [11,40,41]. The base pressure used in our experiments was kept at 1 Torr and a working pressure of 10 Torr was implemented by introducing Ar as the carrier gas. The study of temperature impact led to an optimized 900 °C temperature with a heating time of 1h which is an improvement compared to atmospheric condition. Fig. 3a Shows a low magnification SEM image of the nanowires synthesized on carbon paper. XRD results ( Fig4.3b ) indicate that these nanowires a similar crystal structures as nanostructures synthesized in in atmospheric condition (Cubic CoSi crystal).

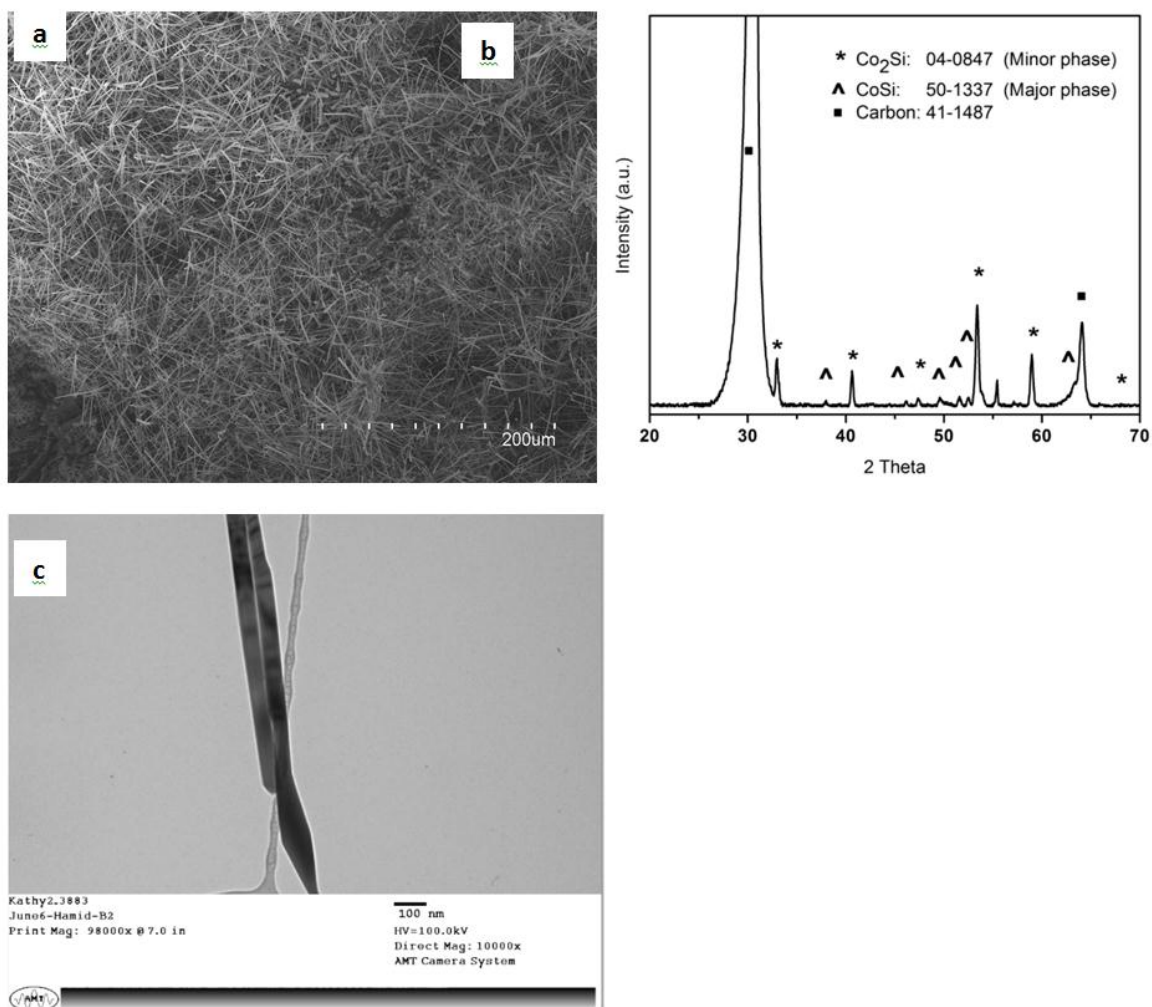


**Figure 5.3 (a) HRSEM at 900 °C at 10 Torr; (b) XRD pattern; (c) TEM image of single nanowire; (d) HRTEM of CoSi nanowire (inset is SAED pattern).**

However, the TEM observations (Fig4.3c) indicate that in contrast to the core-shell structure of the CoSi nanostructures at ambient pressure where the diameter of the crystalline core and amorphous shell were comparable, CoSi nanostructures synthesized at low pressure have a very thin layer and in some nanowires only one phase can be observed. TEM analysis show these nanowires have an average diameter of around 60 nm with lengths up to only a few micrometers.

### 4.3.1. Synthesis Temperature

In addition to CVD chamber pressure, the synthesis temperature plays an important role in determining the morphology of nanostructures deposited on the substrate. Here we will discuss the effect of temperature at two different pressure levels,

1. atmospheric condition
2. pressure level of 10 Torr

Other pressures were also investigated, though these two pressure levels were found to have significant impacts for base pressures above 1 Torr.

#### **Temperature effect at atmospheric condition**

At ambient pressure of 1bar, the effects of wide range of temperatures on the deposited nanostructures were studied. SEM results of temperature conditions of 850 °C, 900 °C and 930 °C can be observed in Fig4. 4a,4b and 4c respectively.

As previously stated, the optimum temperature was found to be 850 °C at the center of the heating zone. EDX spectrum (Fig4.4d) confirms the ratio of Co:Si to be 1:1 which is in agreement with the results obtained by XRD in Fig4.2. At lower temperatures it was found that no deposition of Co would occur on the substrate. This could be the result of insufficient energy for Co deposition at low temperatures.

At high temperatures, around 900 °C, SEM observations (Fig4.4c) indicate the significant reduction in density of nanowires synthesized on the substrate. In addition high magnification SEM images show changes to the morphology of deposited

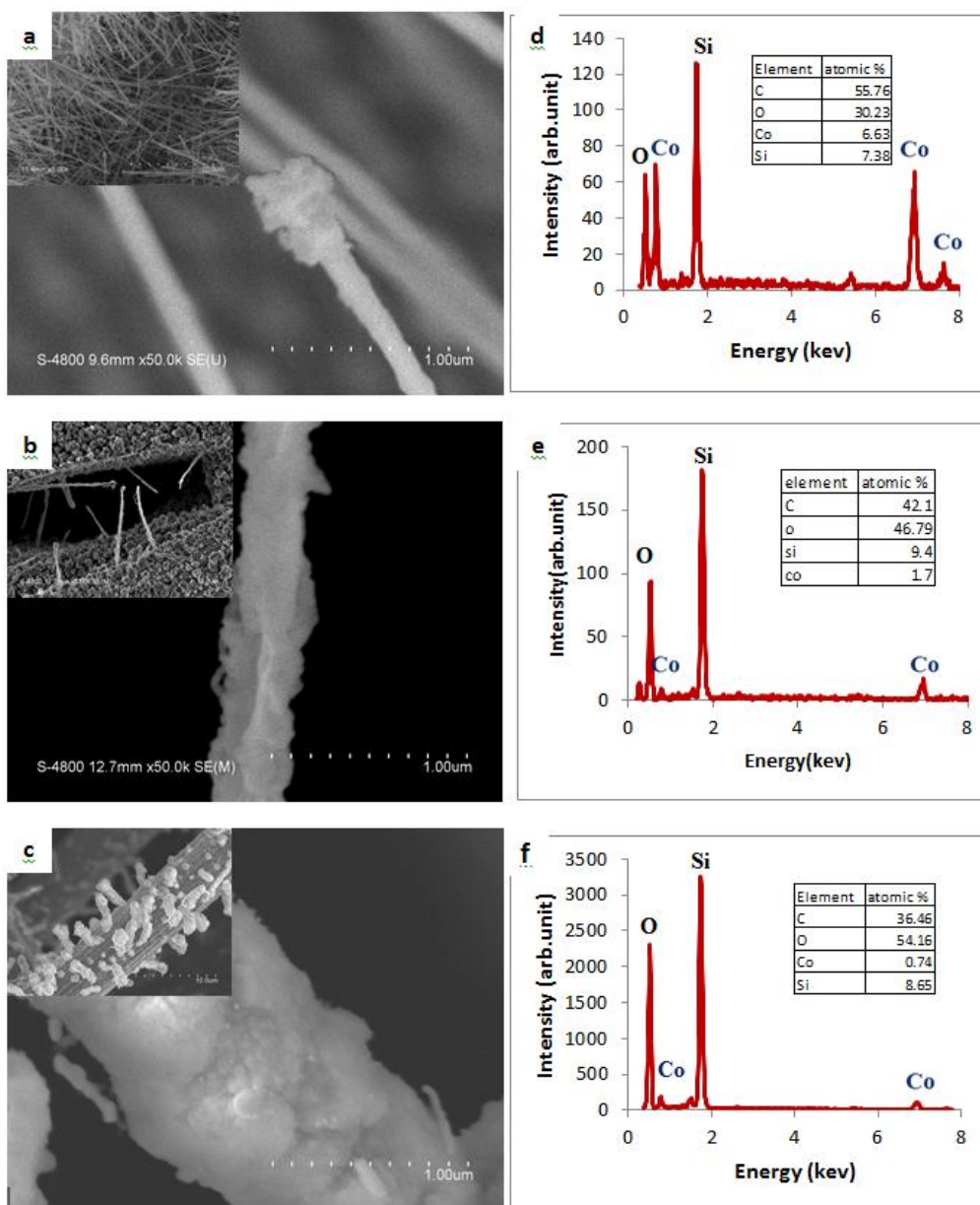


**Figure 5.4** Representative High magnification SEM image (inset is low magnification) of CoSi nanowires synthesized in atmospheric condition at (a) 850 °C , (b) 900 °C and (c) 930°C respectively. at 10 Torr (b) EDX spectrum of products synthesized at (d) 850°C , (e)900°C (f) 930°C

nanowires compared nanostructures deposited at optimum temperatures. This can be due to the high oxidation rate at higher temperatures as it can be seen in Fig4.4b. EDX results (Fig4.4e) illustrate the presence of higher amount of oxygen and silicon and reduction of Co deposition at these temperatures which confirm the higher rate of oxidation of silicon



and Co and the change in the morphology of products at high temperatures. Nonetheless the catalyst particles remain present on the top of the nanowires which conclude that the growth of these nanowires is through VLS process. It was found that the diameter increased to near 400 nm and the morphology of the nanowires had also changed. As it is apparent in EDX spectrum the oxidation is high as well (Fig4.4f).

### **Temperature effect at low pressure condition**

In low pressure condition investigation of the temperature effect on the structure and the morphology of the nanowires was carried out in a temperature range of 850 to 950 °C.

The experiments were carried out using the same CVD furnace.  $\text{CoCl}_2$  was also used as the precursor and silicon powder as the silicon source. The pressure in the CVD process was lowered using a mechanical vacuum pump which brought the base pressure of the system to 1mbar. The working pressure was increased to 10mbar with the introduction of Ar as carrier gas. As a result of lower pressure the evaporation temperature of the precursor would change and the  $\text{CoCl}_2$  precursor was positioned at a lower temperature of 500°C. High resolution SEM images of the products obtained at 3 different temperatures are shown in Fig4.5a, b and c. At temperatures around 850 °C as it is shown in Fig4.5a there were small depositions observed as nanoparticles and nanorods on the substrate which through EDX analysis (Fig4.5d) they were found to be composed of Co and silicon with a ratio of 2:1 . Increasing the temperature to around 900 °C resulted in large production of nanowires on the fibers of the carbon paper. These nanowires as mentioned before are crystalline and have a smaller diameter than the

nanowires produced in atmospheric condition which is due to the lower super saturation at low pressure. EDX results (Fig4.5e) show that the Co and Silicon ratio is 1:1 which is in agreement with the XRD results shown in Fig4. 3c.

As we increase the temperature to over 930 °C it was observed that large cluster of Co and silicon was deposited on the surface over which the growth of the nanowires has occurred. The formation of the clusters means that there is high vapor pressure compared to lower temperatures around the substrate and as result of high temperature the surface energy is reduced which in turn leads to deposition of Co and Silicon in a bulk form on the carbon paper. EDX spectrum of these nanostructures shown in Fig4.5f reveals that they are composed of Co and silicon and oxygen. Though as observed in the spectra the ratio of the Co:Si is 2:1. This type of cluster formation has also been reported by Liang et al., [58] on silicon wafer. They have indicated that the bulk formations of the clusters on the substrate are a crystalline  $\text{Co}_2\text{Si}$  structure, which is in agreement with our results obtained through XRD and EDX analysis.

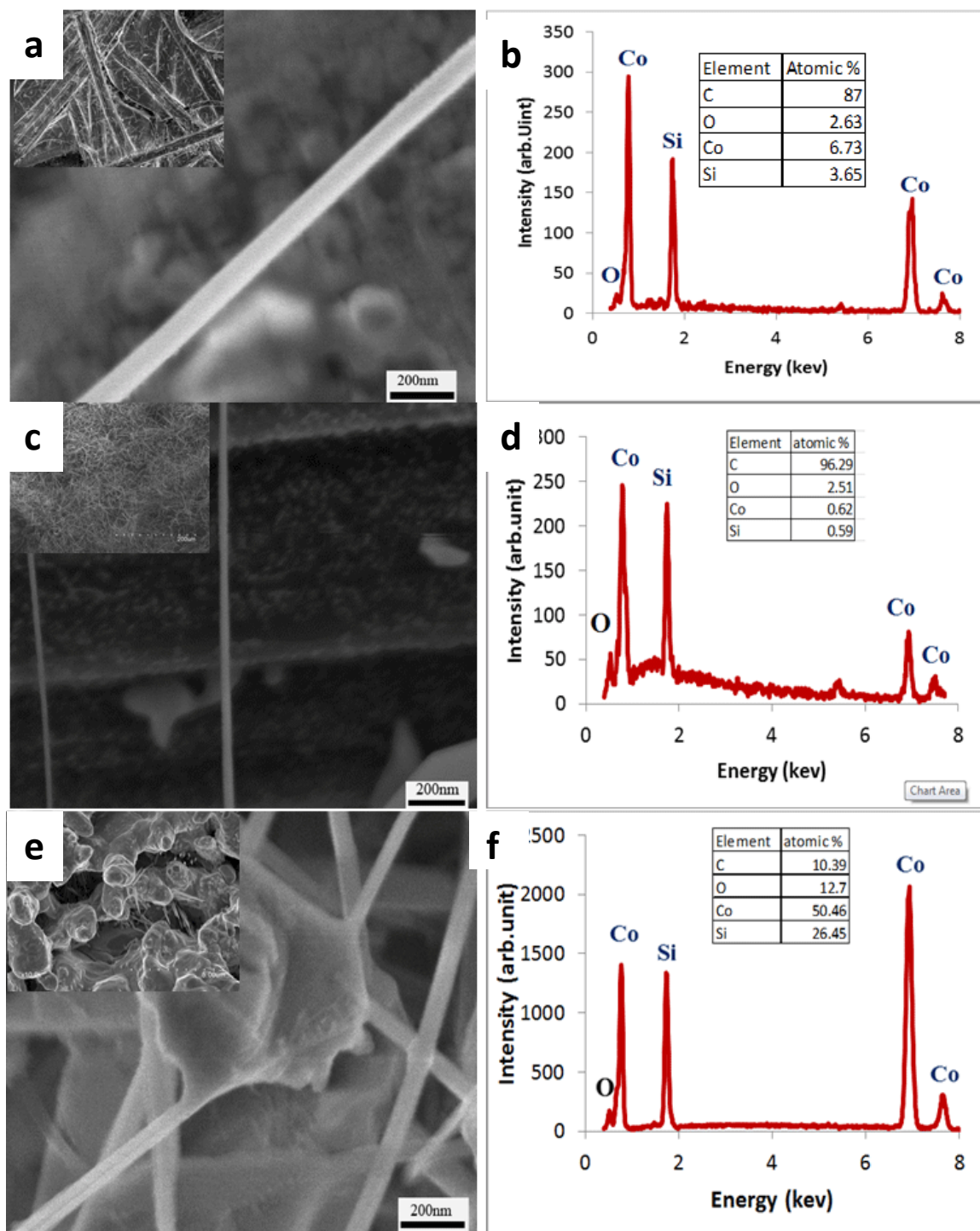


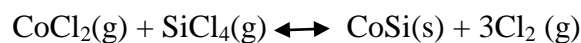
**Figure 5.5** Representative High magnification SEM image (inset is low magnification) of CoSi nanowires synthesized in 1mbar ambient pressure at (a) 850oC , (b) 900oC and (c) 930oC respectively. at 10 Torr (b) EDX spectrum of products synthesized at (d) 850oC , (e) 900°C(f)930°C

### 4.3.2. Growth mechanism

Based on the results of effect of growth parameters on the morphology of nanostructures deposited on the substrate a growth mechanism can be proposed for the synthesis of CoSi nanostructures at two different synthesis pressures. At low pressure as observed in the SEM images the nanowires grow from the clusters formed on the substrate which suggest a VLS mechanism where the agglomerated particles act as the catalyst.

At atmospheric pressure the particles on the tip of the nanowires were analysed through HRTEM and EDX spectrum. Fig4.6a,b shows the low magnification and HRTEM of the nanoparticle on top of a nanowire. As observed two phases are present in the particle as well as the nanowire itself. EDX analysis (Fig4.6.c) reveals the ratio of cobalt and silicon in the particle is 2:1 which is similar to the ratio of the clusters observed at experiments at 1mbar , suggesting the same VLS mechanism.

In this mechanism the  $\text{CoCl}_2$  vapour which is transported to the high temperature zone chemically reacts with the silicon vapour over the substrate. The possible reaction pathway concluded from various experiments and also suggested in previous report [30,40] that leads to the formation of CoSi nanowires is as follows.



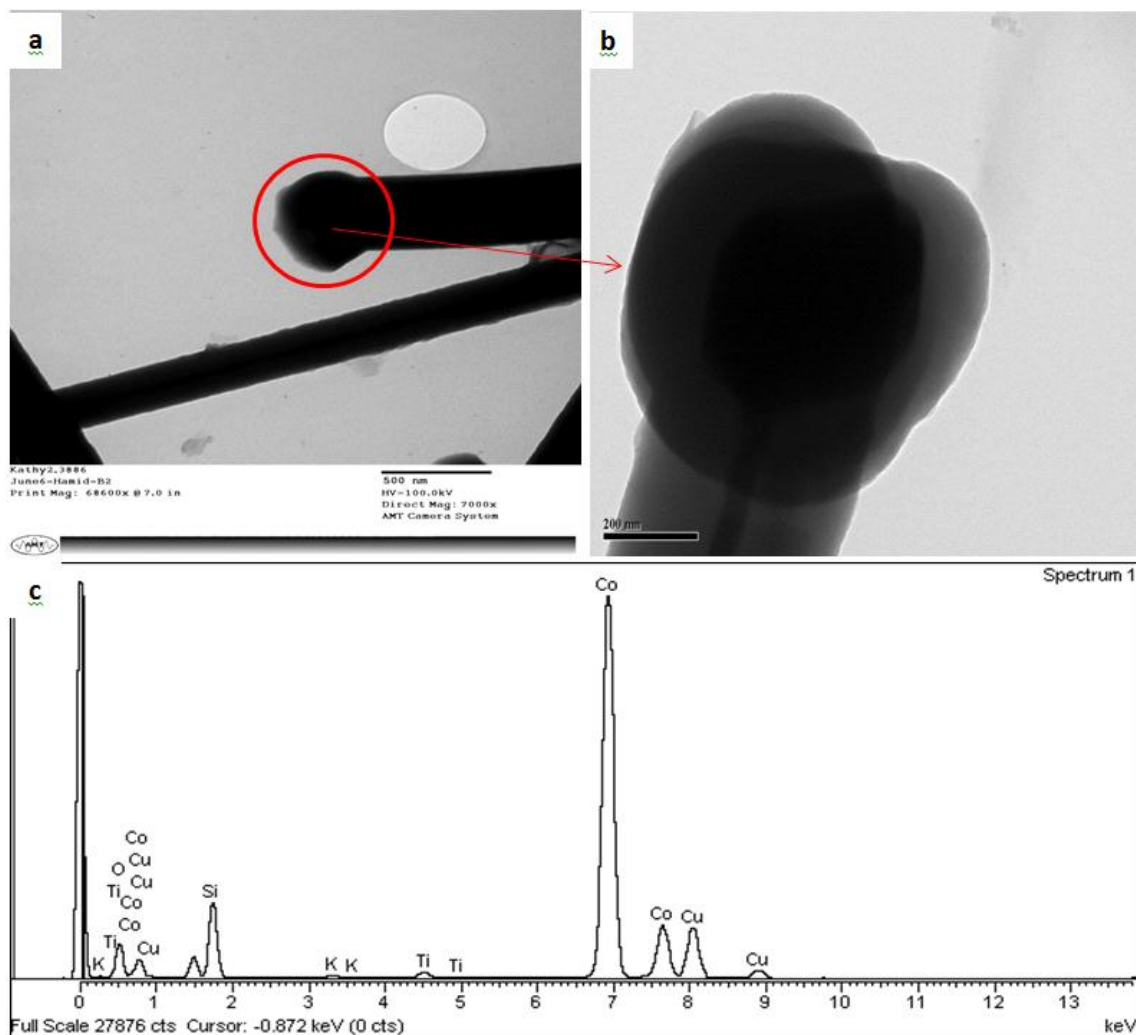
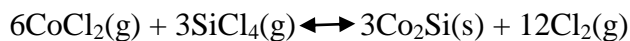


**Figure 5.6** (a) low magnification TEM image of CoSi nanowire with a nanoparticle; (b) High Resolution TEM image of the catalyst nanoparticle; (c) EDX spectra of the nanoparticle.

An optimum rate of reaction at 1mbar and atmospheric pressure controlled by the vapour pressure of the two precursors and the temperature zone of the substrate, results in the formation of NW with specific morphologies at each condition. At low pressure the reaction occur rapidly and as a result the amount of  $\text{CoCl}_2$  and  $\text{SiCl}_4$  produce in a short period which is probable for these gases to enter in the reaction below forming  $\text{Co}_2\text{Si}$  [59].



As reported by Hsia et. al. [60], at temperatures above 850°C, the most stable phase is CoSi and as a result in our experiments the existence of Co<sub>2</sub>Si can only be as a catalyst where the Cobalt atoms diffuse into the deposited silicon elements.

### 4.3. Conclusion

High density CoSi nanowires were synthesized using a single zone CVD process on carbon paper at 1mbar and atmospheric pressure. The nanowires synthesized at high pressure had a core-shell structure with a crystalline CoSi core covered by amorphous SiO<sub>2</sub> layer. In contrast on nanostructures synthesized at low pressures, no or very thin SiO<sub>2</sub> could be found around the CoSi crystalline structures. The effect of temperature on the morphology nanostructures deposited in different synthesis pressures were investigated. Based on these results a VLS growth mechanism using Co<sub>2</sub>Si as catalysts was proposed for the synthesis of CoSi at different pressures.

## References

1. **Cao L M, Tian H, Zhang Z, Feng M, Zhan Z J, Wang W K and Zhang X Y.** 2008 , Cryst. Growth Des., pp. 8, 4350.
2. **Yan K Y, Xue Q Z, Xia D, Chen H J, Xie J and Dong M D.** 2009, ACS Nano, pp. 3,2235.
3. **Zhang Y, Suenaga K, Colliex C and Iijima S.** 1998, science, p. 281 973.
4. **Zhan J H, Bando Y, Hu J Q, Li Y B and Golberg D.** 2004, Chem. matter, p. 16 5158.
5. **Xie Y, Qiao Z P, Chen M, Liu X M and Qian Y T.** 1999 , Adv. matter, p. 11 1512.
6. **Enyashin A. N., Ivanovski A.** 2005, Nanotechnology, p. 16 1304.
7. **Daly B, Arnold D C, Kulkarni J S, Kazakova O, Shaw M T, Nikitenko S, Erts D, Morris M A and Holmes J D.** 2006, small, p. 2 1299.
8. **Crowley T A, Daly B, Morris M A, Erts D, Kazakova O, Boland J J, Wu B and Holmes J D.** 2005, j. Matter chem., p. 15 2408.
9. **Luo Y, Wang L w.** 2010, ACS Nano, p. 491.
10. **Xu J, Lee C S, Tang Y B, Chen X, Chen Z H, Zhang W J, Lee S T, Zhang W X and Yang Z H.** 2010, ACS Nano , p. 4 1845.
11. **C L Hsin, S Y Yu and W W Wu.** 2010, Nanotechnology , p. 485602.
12. **S. L. Zhang, U. Smith, J. Vac.** 2004, Sci. techno., pp. 22 1361-1370.
13. **Maszara, W. P.** 2005, Electrochem. Soc., pp. 152 G550-G555.
14. *semiconducting silicides* . **Borisenko, V. E.** 2000, springer, Berlin, p. vol 39 page 348.
15. **J. Derrien, J. Chevrier, V. Lethanh and J. E. Mahan.** 1992, Appl. Surface Sci., pp. 56-58, 382-393.
16. **Wu Y, Xiang J, Yang C, Lu W and Lieber C M.** 2004, Nature, p. 430 61.
17. **Liu B Z, Wang Y F, Dilts S, Mayer T S and Mohny S E.** 2007, Nanoletter, p. 7 818.
18. **K Kang, K Song, H Heo, S Yoo, G S Kim, G Lee, Y M Kang and M H Jo.** 2011, Chem Sci., pp. 2, 1090.
19. **Zhang S. L., M. Ostling.** 2003, Crit Rev. Solid state Mater. Sci, pp. 28,1.
20. *Silicide Technology for Integrated Circuits.* **Chen, L. J.** 2004, The institution of Electrical Engineering, London, UK.
21. **J, Lur W and Chen L.** 1988, Appl. Physics, p. 64 3505.
22. **Ren W L, Li C C, Zhang L T, Ito K and Wu J S.** 2005, J. Alloys, p. 392 50.

23. **C Tsai, C Y Wang, J Tang, M H Hung, K L. Wang , and L J Chen.** 2011, *J. ACS Nano*, pp. 9552-9558.
24. **J E. Mink, J P. Rojas, B E. Logan, and M M. Hussain.** 2012, *Nano Letter*, pp. 791-795.
25. **J Wu, F Xia, M Pan and X D Zhou.** 2012, *J. of Electrochem. Soc.*, p. 159(6).
26. **H L Zhang, F Li, C Liu and H M Cheng.** 2008, *Nanotechnology* , p. 19 165606.
27. **C K. CHAN, H PENG, G LIU, K McILWRATH, X F ZHANG, R A. HUGGINS AND Y CUI.** 2007, *Nature nanotechnology*, p. 10 1038.
28. **Y. P. Song, A. L. Schmitt, and S. Jin.** 2007, *Nano Lett*, pp. 7(4), 965 .
29. **Y. L. Chueh, M. T. Ko, L. J. Chou, L. J. Chen, C. S. Wu, and C. D. Chen.** 2007, *Nano Lett*, pp. 16(8), 1637.
30. **K Seo, S Lee, H Yoon, J In, K S. K. Varadwaj, Y Jo, M H Jung, J Kim and B Kim.** 2009, *ACS Nano* , pp. Vol3 No 5 ,1145-1150.
31. **k Seo, K. S. K. Varadwaj , P. Mohanty, S. Lee, Y. Jo, M. H. Jung , J. Kim , B. Kim.** 2007, pp. 7, 1240-1245.
32. **S. Zhou, X. Liu, Y. Lin and D. Wang,** *Angew.* 2008, *chem, Int. Ed.* , pp. 47, 7681-7684.
33. **S. Zhou, X. Liu, Y. Lin and D. Wang,**. 2009, *Chem mater*, pp. 21,1023-1027.
34. **Z. Liu, H. Zhang, L. Wang and D. Yang,**. 2008, *Nanotechnology*, pp. 19,375602.
35. **K. S. K. Varadwaj, K. Seo, J. In, P. Mohanty, J. Park and B. Kim.** 2007, *J. Am. Chem. Soc.*, pp. 129,8594-8599.
36. **K. Seo, K. S. K. Varadwaj, D. Cha, J. In, J. Kim, J. Park and B. Kim.** 2007, *J. phys. Chem C*, pp. 111, 9072-9076.
37. **L. Ouyang, E. S. Thrall , M. M. Deshmukh, H Park.** 2006, *Adv. Mater*, pp. 18,1437.
38. **Andrew L. Schmitt, Lei Zhu, Dieter Schmeiâer, F. J. Himpsel, and Song Jin.** 2006, *J. physical of chemistry*, pp. 110, 18141-18146.
39. **Andrew L. Schmitt, Jeremy M. Higgins, and Song Jin.** 2008, *Nano letter*, pp. vol9. No. 3 810-815.
40. **Y H Liang, S Y Yu, C L Hsin, C W Huang, and W W Wu.** 2011, *J. appl. Phys.*, pp. 110,074302.
41. **C. I. Tsai, P. H. Yeh, C. Y. Wang, H. W. Wu, U. S. Chen, M. Y. Lu, W. W. Wu, L. J. Chen, and Z. L. Wang.** 2009, *Cryst. Growth Des.*, p. 9(10)4514.



## Chapter 6 Conclusion and Future Work

### Conclusions:

During the nanotechnology revolution of the past decade, 1D nanowire (NW) materials have attracted prominent attention and gained significant success. Manipulation of size and morphology materials has led to dramatic changes in the way they were used in different applications. Silicon-based materials have been extensively used for many applications such as complementary metal oxide semiconductor (CMOS) devices, thin film coatings and energy applications. For example, a variety of metal silicide nanostructures have been employed for anode materials of the Li ion batteries in order to overcome the challenges of current lithium ion batteries and obtain high capacity.

The main objective of this thesis has been to synthesize two types of silicide nanomaterial,  $\text{NiSi}_x$  and  $\text{CoSi}$ , using CVD method.

The multiple source Synthesis method carried for producing  $\text{NiSi}_x$  and  $\text{CoSi}_x$  using single zone chemical vapour deposition (CVD) provides a better control over the synthesis of nanostructured products. Previous reports have mostly grown the nanowires either only on silicon wafer or a substrate of the other element. Our method allows a wide range of substrate to be used which broadens the scope of the applications of this system. In addition the use of single zone CVD furnace is also favourable for industrial applications because of the low price as opposed to multiple zone systems.

A series of experiments were conducted in this study to synthesize a variety of novel nanostructured  $\text{NiSi}_x$  on silicon wafer, carbon paper and Ni foam. Analysis of the growth conditions required for optimization of nanowires were carried out and explored. The

morphology and crystal structure of the nanowires at different temperatures and substrates were examined and, based on that, conclusions were made for the growth mechanism of the different nanowires synthesized.  $\text{Ni}_2\text{Si}$  nanowires were synthesized on carbon paper and silicon wafer while  $\text{Ni}_{31}\text{Si}_{12}$  was grown on Ni foam. The diameters of the nanowires for carbon paper and silicon wafer were found to be much larger than on Ni foam while their length were grown of smaller scale. The growth mechanisms for all the substrates were found to be via a vapor-solid (VS) system.

Experiments were carried out to synthesize and grow CoSi nanostructures on carbon paper using chemical vapour deposition method at 1 mbar and atmospheric pressure. Optimum conditions were obtained . Effect of temperature was investigated from 800 to 950 °C. At low pressure, the nanowires were crystalline with diameters of around 60 nm and lengths of few micro meters while at atmospheric pressure the dimensions were almost twice their size with diameters ranging from 100-150 nm and lengths of tens of micrometer. The crystal structure at low pressure and high pressure were found to be CoSi for both conditions. The growth mechanism of the nanowires were suggested for both conditions to be a VLS mechanism based on the observation of nanoparticles at the tip of the nanwoires at atmospheric pressure and cluster formation at the bottom of the nanowires at 1mbar.

### **Future work**

Despite the advances demonstrated in this thesis, a large number of challenges still remain. Future work could focus on the following aspects:

- CVD method is a rather difficult method to achieve controlled and desired products. As a result, obtaining high quality nanostructures of materials requires

more attention. In this thesis, we reported the synthesis of  $\text{Ni}_2\text{Si}$  and  $\text{Ni}_{31}\text{Si}_{12}$  without the use of any catalyst. According to our results, there are indications of other minor phases such as  $\text{Ni}_3\text{Si}_2$  as well as  $\text{NiSi}$  on the substrates. In order to grow dense single phase nanostructures, there have been a few reports recently given to find crystal structures of the nuclei of the nanowires. These studies can further be used for growing single phase nanowires without the presence of additional phase on the substrate.

- The  $\text{CoSi}$  and  $\text{NiSi}_x$  NWs that were synthesized in our experiments had a core-shell structure where the shell was an oxide in the case of  $\text{NiSi}$  or an amorphous  $\text{CoSi}$  structure. In order to remove this shell, there have been a number of methods proposed. Some of have used lower pressures as low as 1mTorr. Other solutions such as using a reductive gas such as  $\text{H}_2$  or  $\text{CH}_4$  can be used during the experiments so as to eliminate the oxidation. We have also experimented on using  $\text{NaOH}$  subsequent to the growth to remove the oxide layer. These experiments are still on going to obtain optimum results.
- Battery testing of samples should be carried out to achieve high cycle performance. More substrates such as stainless steel are to be tested in order to examine the stability of the nanowires on the substrate during cycling.

## VITA

<b>Name</b>	Hamid Norouzi Banis
<b>Post-secondary Education and Degrees:</b>	K.N. Toosi University Tehran, Iran 2005-2010 B.Eng.
<b>Honours and Awards:</b>	Ranked 4100 among 1.2 million applicants in nationwide university entrance exam
<b>Related Work Experience</b>	Teaching Assistant The University of Western Ontario 2010-2012

### Publications:

M. Banis, H. Norouzi Banis, Y. Zhang, R. Li, X. Sun, X. Jiang, D. Nikanpour, *Controlled Synthesis and Characterization of Single Crystalline MnO Nanowires and Mn-Si Oxide and their Heterostructures by Vapor Phase Deposition*. **Chem. Phys. Lett.** 501 (2011) 470–474.

H. Norouzi Banis, Y. Zhang, R. Li, X. Sun, Controlled Synthesis and Growth Mechanisms of NiSix Nanowires by Chemical Vapor Deposition. To be submitted

H. Norouzi Banis, Y. Zhang, R. Li, X. Sun, Synthesis of CoSi Nanowires Using Chemical Vapor Deposition at Different Ambient Pressure Levels. To be submitted.